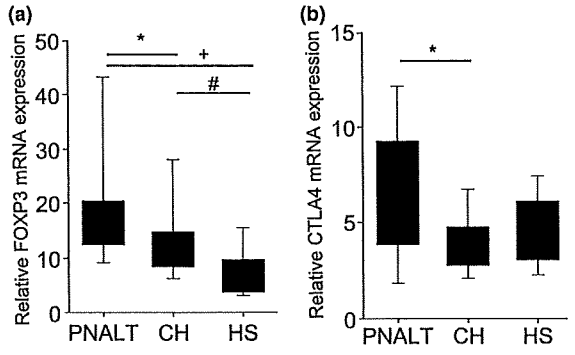

Fig. 2 Comparison of mRNA expression of FOXP3 and CTLA4 in CD4+CD25high+ T cells among the groups. The expression of FOXP3 (a) and CTLA4 (b) in separated CD4+CD25high+ T cells were analysed by real-time reverse transcriptase-polymerase chain reaction as described in Materials and methods. Boxes represent lower and upper quartiles with the median value (solid line) between boxes, while the whiskers represent the minimum and maximum values. *, $P < 0.05$; , $P < 0.01$; +, $P < 0.001$. For definitions of PNALT, CH and HS, see Fig. 1.

production stimulated with antigen-pulsed DC. We compared such responses between samples with or without CD4+CD25+ T cells. In PNALT patients, HCV NS5-specific T cell proliferation or IFN-γ production of CD25-depleted CD4+ T cells was significantly higher than those of the bulk CD4+ T cells (Fig. 3a,b). In contrast, in CH patients, such restoration did not occur significantly even when CD4+ CD25+ T cells had been depleted (Fig. 3a,b). There was no difference in the production of IL-10 and TGF-β between bulk CD4+ T cells and CD25-depleted CD4+ T cells in both CH and PNALT patients (Fig. 3c,d). These results suggest that co-existing CD4+CD25+ T cells play an inhibitory role in the HCV-specific CD4+ T cell response, in which suppression was more potent in the PNALT than in the CH group.

CD127–FOXP3+ cells, regardless of their CD25 expression, are increased in patients with HCV infection

In the analyses of N-Treg, the frequency of CD4+CD25–FOXP3+ T cells in HCV-infected patients was higher than those in the healthy donors (Fig. 1d). These results suggest that CD4+FOXP3+ T cells, regardless of the degree of CD25

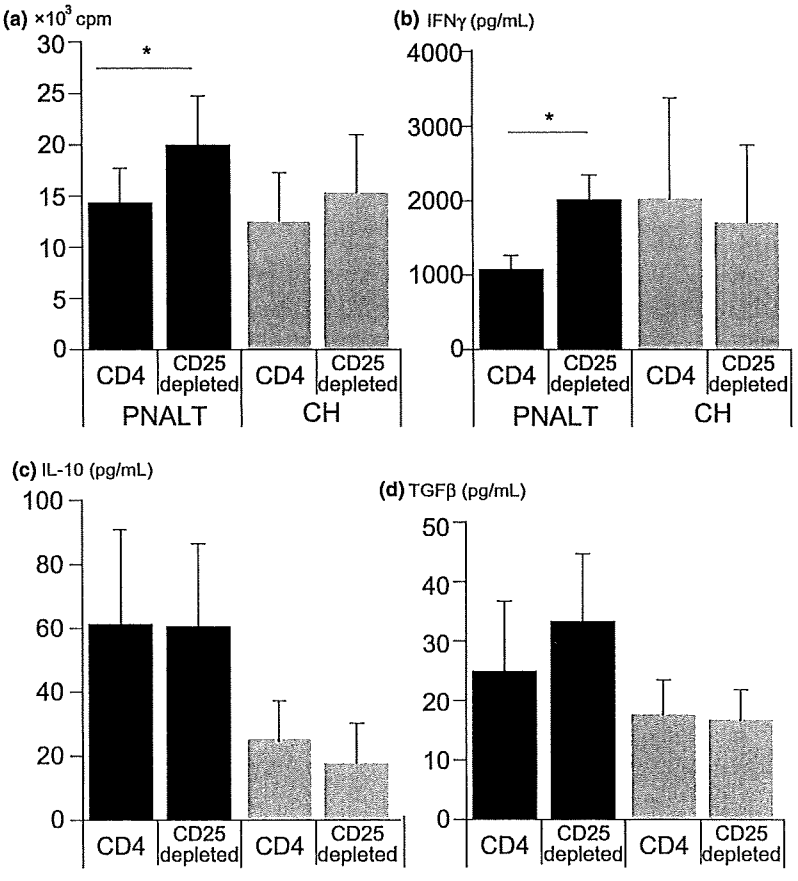

Fig. 3 Changes of hepatitis C virus (HCV)-specific CD4+ T cell responses with or without depletion of CD25+ T cells. Bulk CD4+ T cells or those depleted of CD25+ cells were cultured with autologous monocyte-derived dendritic cells in the presence of HCV-NS5 protein for 5 days as described in Materials and methods. (a) On day 4, [3H]-thymidine was pulsed and the thymidine incorporation was counted with a β-counter. Before the pulsing, the culture supernatants were harvested and subjected to enzyme-linked immunosorbent assay for interferon-γ (b), interleukin-10 (c) and TGF-β (d), respectively. *, $P < 0.05$ by Mann–Whitney *U*-test. For definitions of PNALT and CH, see Fig. 1.

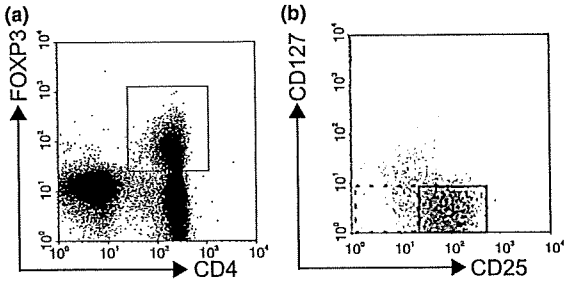

Fig. 4 Gating of CD4+CD127–FOXP3+ cells with variable CD25 expression under FACS analysis. After setting the gate on CD4+FOXP3+ cells [rectangle in the dot plot (a)], were displayed on the CD25 and CD127 axis (b). The presence of CD25+ (bold rectangle) and of CD25– cells (dotted rectangle) in CD4+FOXP3+ cells are shown in plot (b). The frequencies of these cells were analysed.

expression, increase in chronic HCV infection. Alternatively, it implies that higher expression of CD25 is not a universal marker for identifying FOXP3+ cells with regulatory activity. It has been reported that CD127 expression on CD4+ T cells is inversely correlated with FOXP3 expression, suggesting that CD127low/negative cells consist of those with regulatory activity. In order to analyse regulatory T cell subsets more precisely, we first examined FOXP3 expression on CD127– or CD127+ cells paired with CD25 expression in patients with HCV infection (Fig. 4). As a result, the majority of CD4+FOXP3+ T cells belonged to the CD127– population irrespective of CD25 expression (Fig. 4). Next, we compared the frequency of CD4+CD127–FOXP3+ cells, which consist of CD25+ and CD25– cells, among the subject groups (Fig. 5a). The frequency of CD4+CD127–FOXP3+ cells was similar in the CH and the PNALT groups, both of which were significantly higher than those in the HS (Fig. 5a). Finally, in order to estimate the profile of CD4+CD127–FOXP3+ cells according to CD25 expression, we compared the percentage of CD25+CD127–FOXP3+ or CD25–CD127–FOXP3+ cells in CD4+ T cells among the groups. The percentage of CD25+CD127–FOXP3+ T cells in CD4+ T cells was comparable for PNALT and CH (Fig. 5b). In clear contrast, the percentage of CD25–CD127–FOXP3+ T cells in the PNALT was lower than those in the CH (Fig. 5c). The frequencies of these cells were higher in the HCV-infected patients than in HS (Fig. 5b,c). When we set the focus on the proportion of CD25+CD127– or CD25-CD127– cells in the FOXP3+ cells in the periphery as a whole, we found that the proportion of CD25+CD127– cells in the PNALT was higher than that in the CH group (Fig. 5d). On the other hand, the proportion of CD25–CD127– cells in FOXP3+ cells was lower in the PNALT than in the CH group (Fig. 5e). Therefore, the phenotypic profiles of FOXP3+ T cells are distinct between PNALT and CH patients, with regard to the expression of CD127 and CD25.

DISCUSSION

Approximately 30–40% of chronically HCV-infected patients continue to display PNALT for decades. We previously reported the possible contribution of certain human leukocyte antigen haplotypes [23] or DC dysfunction in the maintenance of the PNALT state [24]. However, the precise mechanisms behind this important issue are yet to be

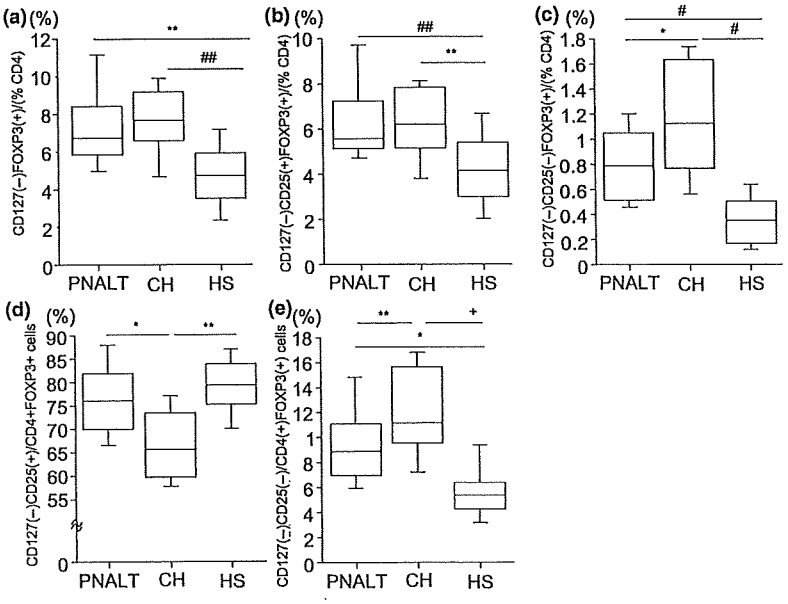

Fig. 5 Comparison in the frequencies of CD127– regulatory T cell subsets among the groups. Frequencies of CD127–FOXP3+ (a), CD127–CD25+FOXP3 (b) and CD127–CD25–FOXP3+ (c) cells among CD4+ T cells were determined by FACS analysis. The proportion of CD127–CD25+ (d) or CD127–CD25– (e) cells in CD4+FOXP3+ cells were also determined. Boxes represent lower and upper quartiles with the median value (solid line) between boxes, while the whiskers represent the minimum and maximum values. *, $P < 0.05$; , $P < 0.01$; **, $P < 0.005$; ##, $P < 0.001$; +, $P < 0.0001$ by Mann–Whitney U-test. For definitions of PNALT, CH and HS, see Fig. 1.

established. Cumulative reports have shown that Th1/Tc1 type responses are instrumental in HCV-induced liver inflammation [7,25,26]. We thus hypothesized that some suppressor mechanisms exist in PNALT patients especially against HCV-specific Th1 and/or CTL reactions.

The involvement of Treg cells in the pathogenesis of various diseases has been reported [9–13]. Most of the studies presented the possibility that N-Treg play substantial roles in the induction of tolerance against aetiological self or nonself antigens, thus leading to alleviation or exacerbation of the disease severity. With regard to HCV infection, several groups have shown that N-Treg are increased both in the periphery and in the liver and are able to inhibit HCV-specific CD4+ or CD8+ T cell responses *in vitro* [17,18,27]. In this study, we showed that the frequency of N-Treg in HCV-infected patients is higher than those in the controls, which is consistent with the previous reports. However, the frequencies of N-Treg are indistinguishable between the patient groups with different disease activities. As for the functional aspect, the deprivation of CD4+CD25+ cells enhanced the HCV NS5-specific CD4+ T cell response in the PNALT than in the CH group, suggesting that co-existing Treg in the PNALT are more suppressive. In addition, the expression of FOXP3 and CTLA4, which are key molecules of the suppressor function, is higher in PNALT than in those with active hepatitis. Venken *et al.* [28] demonstrated that the degree of FOXP3 expression at the single-cell level of N-Treg is well correlated with their suppressive ability, which is supportive of our results. In contrast, Bolacchi *et al.* [29] reported that the frequency of TGF-β+ N-Treg in the PNALT was higher than in the hepatitis group. Furthermore, their frequency was inversely correlated with the histological inflammatory grade, suggesting that TGF-β+ Treg play active roles in alleviating hepatitis. The reasons for the lack of correlation between N-Treg and serum ALT or HCV RNA quantity in the present study may be because of the difference in the target of analyses, such as either peripheral or intra-hepatic Treg, or either TGF-β+ or bulk Treg. Further analyses need to be performed on these important issues, as CD4+FOXP3+ Treg are reported to accumulate more in the portal tract of HCV-infected livers compared with those in the periphery [20].

During the observation period, about 30–40% of PNALT patients began to show elevated or fluctuating ALT abnormalities. What crucial factor triggers HCV-induced liver inflammation remains unknown. One of the plausible explanations is an antigenic shift accompanied by the occurrence of mutations in the HCV genome. In other words, hepatitis may flare up if the mutation raises HCV immunogenicity. Comprehensive analyses of HCV epitopes for CTL using overlapping peptides have shown that the HCV core and NS3 are more immunogenic than the remaining regions; however, the presence of an epitope hierarchy in Treg induction has been controversial. Li *et al.* [30] reported the possibility that Treg are expandable in response to certain epitopes in HCV proteins. In two patients in whom we observed flare-up of hepatitis in this study, we were able to find that the expression of FOXP3 in N-Treg was high in the PNALT status, but declined in the active hepatitis stage (data not shown). Although it is difficult to state whether such phenotypic changes in N-Treg are the cause or the consequence of disease progression, these results suggest the involvement of N-Treg in the degree of HCV-mediated hepatitis. Further detailed study is needed to examine whether or not such changes in N-Treg are related to the sequence evolution in HCV genomes.

Recent research has disclosed that distinct types of Treg are present in humans. Currently, it is generally accepted that CD25+FOXP3+ is the most reliable marker for Treg, which is induced in parallel with the acquisition of suppressor ability. However, owing to the lack of phenotypic markers for specifically identifying adaptive Treg, their roles in clinical settings have been unclear. In this study, CD4+FOXP3+ cells increased in HCV-infected patients, who were either positive or negative for CD25. In contrast to thymus-derived N-Treg expressing a greater degree of CD25, adaptive Treg are presumed to be induced in the periphery with a lesser degree of CD25 expression. Thus, it is likely that CD4+CD25–FOXP3+ T cells in HCV infection contain some part of adaptive Treg.

Treg have been reported to express low levels of CD127 at their cell surface [31]. Furthermore, the expression of CD127 is inversely correlated with FOXP3 expression and with the suppressive function of CD25high+ Treg. Liu *et al.* [22] pointed out the possibility that adaptive Treg are grouped into CD127– cells, which also include FOXP3-negative Tr1 or Th3 cells. Alternatively, You *et al.* [32] reported that murine CD4+CD25lowFOXP3+ T cells might be adaptive Treg, which exert a TGFβ-dependent suppressive function. Taking these reports into consideration, and in order to exclude activated CD25+ T cells, we examined CD4+CD127–CD25–FOXP3+ cells tentatively determined as part of adaptive Treg. In order to confirm that CD4+CD127– cells possess suppressive capacity, we co-cultured sorted CD4+CD127–CD25– or CD4+CD127–CD25+ cells with allogeneic CD4+ T cells stimulated with anti-CD3 and anti-CD28 antibodies. As a result, we found that CD4+CD127– cells, regardless of CD25 expression, significantly suppressed the proliferation of responder CD4+ T cells (manuscript in preparation). Of note is the finding that the frequency of CD127–CD25–FOXP3+ cells is higher in patients with active hepatitis than those in the PNALT group. One of the plausible explanations for such an increase of Treg is the compensatory mechanisms for the aggravation of liver inflammation. In support of this possibility, Bonelli *et al.* [33] reported that CD4+CD127–CD25– cells are increased in patients with systemic lupus erythematosus (SLE), the numbers of which are well correlated with disease activity. With regard to the ability of Treg in SLE patients, CD4+CD127–CD25– cells were potent in the inhibition of T

cell proliferation but not in IFN-γ release. Such a defective suppressor capacity may result in the continuation of tissue inflammation regardless of the presence of abundant Treg. The other conceivable role of CD4+CD25–CD127–FOXP3+ cells in active hepatitis may be a peripheral reservoir of CD4+CD25+FOXP3+ cells in case of flare-up of liver inflammation. In mice, it has been reported that CD25–FOXP3+ cells revert to CD25+FOXP3+ cells upon activation signals, thus leading to the expansion of the Treg pool [34]. In order to reach a definite conclusion on the role of CD127–CD25–FOXP3+ cells, further analyses are needed to elucidate whether these cells are inhibitory to either HCV-specific or HCV-nonspecific T cell responses.

Large-scale studies with HCV-infected patients demonstrated that the cumulative incidence of HCC in the PNALT group is extremely low compared with that in patients with apparent hepatitis and liver cirrhosis [35]. The lesser HCC incidence is also evident in patients who attained a lasting biochemical response to IFN-based therapy; even if they had failed to achieve sustained virological response [36]. These results clearly indicate that the maintenance of the PNALT state is one of the surrogate therapeutic goals in chronic HCV infection. Therefore, it is necessary to clarify the mechanisms of Treg induction in HCV infection, whether they are naturally or adaptively introduced, and to establish a feasible modality for controlling Treg. Our study has shown the importance of subset-oriented analyses of Treg for gaining access to that goal.

ACKNOWLEDGEMENT

This study was funded in part by Ministry of Education, Culture, Sports, Science and Technology, Ministry of Health, Labor and Welfare of Japan.

CONFLICT OF INTEREST

All of the authors do not have any commercial or other association that might pose a conflict of interest.

REFERENCES

1 Kasahara A, Hayashi N, Mochizuki K *et al.* Risk factors for hepatocellular carcinoma and its incidence after interferon treatment in patients with chronic hepatitis C. Osaka Liver Disease Study Group. *Hepatology* 1998; 27(5): 1394–1402.
2 Marcellin P, Levy S, Erlinger S. Therapy of hepatitis C: patients with normal aminotransferase levels. *Hepatology* 1997; 26 (3 Suppl. 1): 133S–136S.
3 Tassopoulos NC. Treatment of patients with chronic hepatitis C and normal ALT levels. *J Hepatol* 1999; 31 (Suppl. 1): 193–196.
4 Persico M, Persico E, Suozzo R *et al.* Natural history of hepatitis C virus carriers with persistently normal aminotransferase levels. *Gastroenterology* 2000; 118(4): 760–764.
5 Suruki R, Hayashi K, Kusumoto K *et al.* Alanine aminotransferase level as a predictor of hepatitis C virus-associated hepatocellular carcinoma incidence in a community-based population in Japan. *Int J Cancer* 2006; 119(1): 192–195.
6 Nelson DR, Marousis CG, Davis GL *et al.* The role of hepatitis C virus-specific cytotoxic T lymphocytes in chronic hepatitis C. *J Immunol* 1997; 158(3): 1473–1481.
7 Schirren CA, Jung MC, Gerlach JT *et al.* Liver-derived hepatitis C virus (HCV)-specific CD4(+) T cells recognize multiple HCV epitopes and produce interferon gamma. *Hepatology* 2000; 32(3): 597–603.
8 Sakaguchi S. Naturally arising CD4+ regulatory T cells for immunologic self-tolerance and negative control of immune responses. *Annu Rev Immunol* 2004; 22: 531–562.
9 Viglietta V, Baecher-Allan C, Weiner HL, Hafler DA. Loss of functional suppression by CD4+CD25+ regulatory T cells in patients with multiple sclerosis. *J Exp Med* 2004; 199(7): 971–979.
10 Ehrenstein MR, Evans JG, Singh A *et al.* Compromised function of regulatory T cells in rheumatoid arthritis and reversal by anti-TNFalpha therapy. *J Exp Med* 2004; 200(3): 277–285.
11 Sugiyama H, Gyulai R, Toichi E *et al.* Dysfunctional blood and target tissue CD4+CD25high regulatory T cells in psoriasis: mechanism underlying unrestrained pathogenic effector T cell proliferation. *J Immunol* 2005; 174(1): 164–173.
12 Weiss L, Donkova-Petrini V, Caccavelli L, Balbo M, Carbonneil C, Levy Y. Human immunodeficiency virus-driven expansion of CD4+CD25+ regulatory T cells, which suppress HIV-specific CD4 T-cell responses in HIV-infected patients. *Blood* 2004; 104(10): 3249–3256.
13 Ormandy LA, Hillemann T, Wedemeyer H, Manns MP, Greten TF, Korangy F. Increased populations of regulatory T cells in peripheral blood of patients with hepatocellular carcinoma. *Cancer Res* 2005; 65(6): 2457–2464.
14 Jonuleit H, Schmitt E. The regulatory T cell family: distinct subsets and their interrelations. *J Immunol* 2003; 171(12): 6323–6327.
15 Hori S, Nomura T, Sakaguchi S. Control of regulatory T cell development by the transcription factor Foxp3. *Science* 2003; 299(5609): 1057–1061.
16 Fontenot JD, Rudensky AY. A well adapted regulatory contrivance: regulatory T cell development and the forkhead family transcription factor Foxp3. *Nat Immunol* 2005; 6(4): 331–337.
17 Cabrera R, Tu Z, Xu Y *et al.* An immunomodulatory role for CD4(+)CD25(+) regulatory T lymphocytes in hepatitis C virus infection. *Hepatology* 2004; 40(5): 1062–1071.
18 Rushbrook SM, Ward SM, Unitt E *et al.* Regulatory T cells suppress *in vitro* proliferation of virus-specific CD8+ T cells during persistent hepatitis C virus infection. *J Virol* 2005; 79(12): 7852–7859.
19 Sugimoto K, Ikeda F, Stadanlick J, Nunes FA, Alter HJ, Chang KM. Suppression of HCV-specific T cells without differential hierarchy demonstrated *ex vivo* in persistent HCV infection. *Hepatology* 2003; 38(6): 1437–1448.
20 Ward SM, Fox BC, Brown PJ *et al.* Quantification and localisation of FOXP3+ T lymphocytes and relation to

hepatic inflammation during chronic HCV infection. *J Hepatol* 2007; 47(3): 316–324.
21 Chen W, Jin W, Hardegen N *et al.* Conversion of peripheral CD4+CD25– naive T cells to CD4+CD25+ regulatory T cells by TGF-beta induction of transcription factor Foxp3. *J Exp Med* 2003; 198(12): 1875–1886.
22 Liu W, Putnam AL, Xu-Yu Z *et al.* CD127 expression inversely correlates with FoxP3 and suppressive function of human CD4+ Treg cells. *J Exp Med* 2006; 203(7): 1701–1711.
23 Kuzushita N, Hayashi N, Moribe T *et al.* Influence of HLA haplotypes on the clinical courses of individuals infected with hepatitis C virus. *Hepatology* 1998; 27(1): 240–244.
24 Kanto T, Inoue M, Miyazaki M *et al.* Impaired function of dendritic cells circulating in patients infected with hepatitis C virus who have persistently normal alanine aminotransferase levels. *Intervirology* 2006; 49(1–2): 58–63.
25 Leroy V, Vigan I, Mosnier JF *et al.* Phenotypic and functional characterization of intrahepatic T lymphocytes during chronic hepatitis C. *Hepatology* 2003; 38(4): 829–841.
26 Penna A, Missale G, Lamonaca V *et al.* Intrahepatic and circulating HLA class II-restricted, hepatitis C virus-specific T cells: functional characterization in patients with chronic hepatitis C. *Hepatology* 2002; 35(5): 1225–1236.
27 Boettler T, Spangenberg HC, Neumann-Haefelin C *et al.* T cells with a CD4+CD25+ regulatory phenotype suppress *in vitro* proliferation of virus-specific CD8+ T cells during chronic hepatitis C virus infection. *J Virol* 2005; 79(12): 7860–7867.
28 Venken K, Hellings N, Thewissen M *et al.* Compromised CD4+ CD25(high) regulatory T-cell function in patients with relapsing-remitting multiple sclerosis is correlated with a reduced frequency of FOXP3-positive cells and reduced FOXP3 expression at the single-cell level. *Immunology* 2008; 123(1): 79–89.
29 Bolacchi F, Sinistro A, Ciaprini C *et al.* Increased hepatitis C virus (HCV)-specific CD4+CD25+ regulatory T lymphocytes and reduced HCV-specific CD4+ T cell response in HCV-infected patients with normal versus abnormal alanine aminotransferase levels. *Clin Exp Immunol* 2006; 144(2): 188–196.
30 Li S, Jones KL, Woollard DJ *et al.* Defining target antigens for CD25+ FOXP3+ IFN-gamma-regulatory T cells in chronic hepatitis C virus infection. *Immunol Cell Biol* 2007; 85(3): 197–204.
31 Seddiki N, Santner-Nanan B, Martinson J *et al.* Expression of interleukin (IL)-2 and IL-7 receptors discriminates between human regulatory and activated T cells. *J Exp Med* 2006; 203(7): 1693–1700.
32 You S, Leforban B, Garcia C, Bach JF, Bluestone JA, Chatenoud L. Adaptive TGF-beta-dependent regulatory T cells control autoimmune diabetes and are a privileged target of anti-CD3 antibody treatment. *Proc Natl Acad Sci USA* 2007; 104(15): 6335–6340.
33 Bonelli M, Savitskaya A, Steiner CW, Rath E, Smolen JS, Scheinecker C. Phenotypic and functional analysis of CD4+CD25– Foxp3+ T cells in patients with systemic lupus erythematosus. *J Immunol* 2009; 182(3): 1689–1695.
34 Zelenay S, Lopes-Carvalho T, Caramalho I, Moraes-Fontes MF, Rebelo M, Demengeot J. Foxp3+ CD25– CD4 T cells constitute a reservoir of committed regulatory cells that regain CD25 expression upon homeostatic expansion. *Proc Natl Acad Sci USA* 2005; 102(11): 4091–4096.
35 Okanoue T, Makiyama A, Nakayama M *et al.* A follow-up study to determine the value of liver biopsy and need for antiviral therapy for hepatitis C virus carriers with persistently normal serum aminotransferase. *J Hepatol* 2005; 43(4): 599–605.
36 Tanaka H, Tsukuma H, Kasahara A *et al.* Effect of interferon therapy on the incidence of hepatocellular carcinoma and mortality of patients with chronic hepatitis C: a retrospective cohort study of 738 patients. *Int J Cancer* 2000; 87(5): 741–749.

Mcl-1 and Bcl-xL Cooperatively Maintain Integrity of Hepatocytes in Developing and Adult Murine Liver

Hayato Hikita,[1]* Tetsuo Takehara,[1]* Satoshi Shimizu,[1] Takahiro Kodama,[1] Wei Li,[1] Takuya Miyagi,[1] Atsushi Hosui,[1] Hisashi Ishida,[1] Kazuyoshi Ohkawa,[1] Tatsuya Kanto,[1] Naoki Hiramatsu,[1] Xiao-Ming Yin,[2] Lothar Hennighausen,[3] Tomohide Tatsumi,[1] and Norio Hayashi[1]

Anti-apoptotic members of the Bcl-2 family, including Bcl-2, Bcl-xL, Mcl-1, Bcl-w and Bfl-1, inhibit the mitochondrial pathway of apoptosis. Bcl-xL and Mcl-1 are constitutively expressed in the liver. Although previous research established Bcl-xL as a critical apoptosis antagonist in differentiated hepatocytes, the significance of Mcl-1 in the liver, especially in conjunction with Bcl-xL, has not been clear. To examine this question, we generated hepatocyte-specific Mcl-1–deficient mice by crossing *mcl-1*$^{flox/flox}$ mice and *AlbCre* mice and further crossed them with *bcl-x*$^{flox/flox}$ mice, giving Mcl-1/Bcl-xL–deficient mice. The *mcl-1*$^{flox/flox}$ *AlbCre* mice showed spontaneous apoptosis of hepatocytes after birth, as evidenced by elevated levels of serum alanine aminotransferase (ALT) and caspase-3/7 activity and an increased number of terminal deoxynucleotidyl transferase-mediated 2′-deoxyuridine 5′-triphosphate nick-end labeling (TUNEL)-positive cells in the liver; these phenotypes were very close to those previously found in hepatocyte-specific Bcl-xL–deficient mice. Although *mcl-1*$^{flox/+}$ *AlbCre* mice did not display apoptosis, their susceptibility to Fas-mediated liver injury significantly increased. Further crossing of Mcl-1 mice with Bcl-xL mice showed that *bcl-x*$^{flox/+}$ *mcl-1*$^{flox/+}$ *AlbCre* mice also showed spontaneous hepatocyte apoptosis similar to Bcl-xL–deficient or Mcl-1–deficient mice. In contrast, *bcl-x*$^{flox/flox}$ *mcl-1*$^{flox/+}$ *AlbCre*, *bcl-x*$^{flox/+}$ *mcl-1*$^{flox/flox}$ *AlbCre*, and *bcl-x*$^{flox/flox}$ *mcl-1*$^{flox/flox}$ *AlbCre* mice displayed a decreased number of hepatocytes and a reduced volume of the liver on day 18.5 of embryogenesis and rapidly died within 1 day after birth, developing hepatic failure evidenced by increased levels of blood ammonia and bilirubin. *Conclusion:* Mcl-1 is critical for blocking apoptosis in adult liver and, in the absence of Bcl-xL, is essential for normal liver development. Mcl-1 and Bcl-xL are two major anti-apoptotic Bcl-2 family proteins expressed in the liver and cooperatively control hepatic integrity during liver development and in adult liver homeostasis in a gene dose-dependent manner. (HEPATOLOGY 2009;50:1217-1226.)

See Editorial on Page 1009

Abbreviations: ALT, alanine aminotransferase; PCR, polymerase chain reaction; RT-PCR, reverse transcription polymerase chain reaction; TNF-α, tumor necrosis factor alpha; TUNEL, terminal deoxynucleotidyl transferase-mediated 2′-deoxyuridine 5′-triphosphate nick-end labeling.

From the [1]Department of Gastroenterology and Hepatology, Osaka University Graduate School of Medicine, Osaka, Japan; the [2]Department of Pathology, University of Pittsburgh School of Medicine, Pittsburgh, PA; and the [3]Laboratory of Genetics and Physiology, National Institute of Diabetes and Digestive and Kidney Diseases, National Institutes of Health, Bethesda, MD.

**These authors contributed equally to this work and share first authorship.*

Received January 31, 2009; accepted June 8, 2009.

Supported in part by a Grant-in-Aid for Scientific Research from the Ministry of Education, Culture, Sports, Science, and Technology, Japan (to T.Tak.).

Address reprint requests to: Norio Hayashi, M.D., Ph.D., Department of Gastroenterology and Hepatology, Osaka University Graduate School of Medicine, 2-2 Yamadaoka, Suita, Osaka 565-0871, Japan. E-mail: hayashin@gh.med.osaka-u.ac.jp; fax:

Published online in Wiley InterScience (www.interscience.wiley.com).

DOI 10.1002/hep.23126

Potential conflict of interest: Nothing to report.

Additional Supporting Information may be found in the online version of this article.

The mitochondrial pathway of apoptosis is regulated by the Bcl-2 family proteins.[1,2] They are functionally divided into two basic groups: pro-apoptotic and anti-apoptotic members. Pro-apoptotic members are further divided into multi-domain members, such as Bax and Bak, and BH3-only proteins. Bax/Bak triggers release from mitochondria of cytochrome c, presumably by forming pores at the mitochondrial outer membrane. Cytochrome c released into the cytosol activates multiple caspases, which cut a variety of cellular substrates and dismantle the cell.[3] The release of Bax/Bak–mediated cytochrome c is considered to be a point of no return and a commitment to cell death.[4] Killing by BH3-only proteins, such as Bid, Bim, or Puma, requires Bax or Bak, placing them upstream of Bak/Bax activation. BH3-only proteins are transcriptionally or posttranslationally activated by a variety of cellular stresses. They are considered to be sensors that transmit apoptotic stimuli to mitochondria. Anti-apoptotic members, including Bcl-2, Bcl-xL, Mcl-1, Bcl-w, and Bfl-1, inhibit the mitochon-

drial pathway of apoptosis either by directly blocking Bak/Bax activation or by sequestering BH3-only proteins from Bak or Bax.

Mcl-1 has increasingly attracted attention because of its role in liver disease. Several reports have shown that Mcl-1 is overexpressed in a subset of human hepatocellular carcinomas and provides apoptosis resistance.[5-7] The multi-kinase inhibitor sorafenib, which was recently approved by the Food and Drug Administration as a chemotherapeutic agent for hepatocellular carcinoma,[8] is capable of down-regulating Mcl-1 expression and producing apoptosis in hepatoma cells.[9] Cycloxygenase 2 or hepatocyte growth factor up-regulates Mcl-1 expression in hepatocytes and improves Fas-mediated liver injury.[10,11] Recently, enforced expression of Mcl-1 was reported to reduce liver injury induced by anti-Fas injection in mice.[12] However, little is known about the physiologic significance of Mcl-1 in hepatocytes.

We previously reported that hepatocyte-specific Bcl-xL knockout mice were born and grew up but developed spontaneous hepatocyte apoptosis, identifying Bcl-xL as a critical apoptosis antagonist in hepatocytes.[13] This raises a question of whether other anti-apoptotic Bcl-2 family members, such as Mcl-1, have a significant role in regulating hepatocyte apoptosis and what the relationship is among those molecules. To this end, in the current study, we generated hepatocyte-specific Mcl-1 knockout as well as Bcl-xL/Mcl-1 double knockout mice and found that, like Bcl-xL, Mcl-1 is critical for maintaining hepatocyte integrity in adult liver, but not essential for liver development. However, both deficiencies cause a severe defect in liver development and lethality during the early neonatal period because of severe hepatic failure. The current study identifies Bcl-xL and Mcl-1 as two major anti-apoptotic Bcl-2 family proteins in the liver and demonstrates their gene dose–dependent effects for controlling hepatic integrity.

Materials and Methods

Mice. Mice carrying the *mcl-1* gene encoding amino acids 1 through 179 flanked by 2 *lox*P (*mcl-1*$^{flox/flox}$) were provided by Dr. You-Wen He of Duke University.[14] Mice carrying a *bcl-x* gene with two *lox*P sequencers at the promoter region and a second intron (*bcl-x*$^{flox/flox}$) were described previously.[15] Heterozygous AlbCre transgenic mice expressing Cre recombinase gene under the promoter of the albumin gene were described previously.[13] We generated hepatocyte-specific Mcl-1 knockout mice (*mcl-1*$^{flox/floox}$ *AlbCre*) by mating *mcl-1*$^{flox/flox}$ and *AlbCre* mice. We then used these knockout mice to generate hepatocyte-specific Bcl-xL/Mcl-1 knockout mice (*bcl-x*$^{flox/flox}$ *mcl-1*^{floxflox} *AlbCre*) by mating them with *bcl-x*$^{flox/flox}$ mice. Traditional Bid knockout mice were described previously.[16] They were maintained in a specific pathogen–free facility and treated with humane care under approval from the Animal Care and Use Committee of Osaka University Medical School.

Genotyping. Genomic DNA was extracted from the tail and subjected for polymerase chain reaction (PCR) for genotyping mice. The primers used were as follows: 5′-GCCACCTCATCAGTCGGG-3′ and 5′-TCAGAAGCCGCAATATCCCC-3′ for the *bcl-x* allele; 5′-GGTTCCCTGTCTCCTTACTTACTGTAG-3′ and 5′-CTCCTAACCACTGTTCCTGACATCC-3′ for the *mcl-1* allele; 5′-GCGGTCTGGCAGTAAAAACTATC-3′, 5′-GTGAAACAGCATTGCTGTCACTT-3′, 5′CTAGGCCACAGAATTGAAAGATCT-3′ 5′-GTAGGTGGAAATTCTAGCATCATCC-3′ for the *AlbCre* allele; 5′-CCGAAA TGTCCCATAAGAG-3′, 5′-GAGATGGACCACAACATC-3′, and 5′ TGCTACTTCCATTTGTCACGTCCT-3′ for the *bid* allele. PCR products were electrophoretically separated using 2% agarose gels. The expected sizes of the PCR products were as follows: 165 bp for the wild-type *bcl-x* allele, 195 bp for the floxed *bcl-x* allele, 200 bp for the wild-type *mcl-1* allele, 300 bp for the floxed *mcl-1* allele, 130 bp for the wild-type *bid* allele, and 350 bp for the *bid* knockout allele. *AlbCre*-negative mice showed a 350-bp band, and heterozygous *AlbCre* mice showed 100-bp and 350-bp double bands.

Apoptosis Assay. To measure serum ALT level and caspase-3/7 activity, blood was collected from the inferior vena cava of mice and centrifuged. Serum was stored at −20°C until use. Serum ALT levels were measured by a standard method at Oriental Kobo Life Science Laboratory (Nagahama, Japan), and serum caspase-3/7 activity was measured by a luminescent substrate assay for caspase-3 and caspase-7 (Caspase-Glo assay, Promega, Tokyo, Japan). For histological analysis, livers were formalin-fixed, embedded in paraffin, and thin sliced. The liver sections were stained with hematoxylin-eosin. To detect cells with oligonucleosomal DNA breaks, the sections were also subjected to terminal deoxynucleotidyl transferase-mediated 2′-deoxyuridine 5′-triphosphate nick-end labeling (TUNEL) staining, according to a previously reported procedure.[17] For Fas-stimulating study, anti-Fas antibody (Jo2 clone) (PharMingen, San Diego, CA) was intraperitoneally injected into mice 3 hours before sacrifice.

Western Blot Analysis. Approximately 25 mg liver tissues was lysed with a lysis buffer (1% NP-40, 0.5%

sodium deoxycholate, 0.1% sodium dodecyl sulfate and 1× protein inhibitor cocktail (Nacalai tesque, Kyoto, Japan), phosphate-buffered saline; pH 7.4). After incubation on ice for 15 minutes, the lysate was centrifuged at 10,000*g* for 15 minutes at 4°C. The protein content of the supernatants was determined using a bicinchoninic acid protein assay kit (Pierce, Rockford, IL). Equal amounts of protein were electrophoretically separated by sodium dodecyl sulfate polyacrylamide gels (8% or 12%) and transferred onto polyvinylidene fluoride membrane. For immunodetection, the following antibodies were used: anti–Bcl-xL antibody (Santa Cruz Biotechnology, Santa Cruz, CA), anti–Mcl-1 antibody (Rockland, Gilbertsville, PA), anti-Bax antibody (Cell Signaling Technology, Beverly, MA), anti-Bid antibody (Cell Signaling Technology), anti-albumin antibody (Affinity Bioreagents, Golden, CO), and anti–beta actin antibody (Sigma-Aldrich, Saint Louis, MO). Detection of immunolabeled proteins was performed using a chemiluminescent substrate (Pierce).

Neonate Analysis. Neonatal mice delivered by cesarean section were suckled by a surrogate mother and sacrificed at 10 hours after birth. Blood from the neonatal mice was centrifuged, and the plasma was stored at −20°C until use. The levels of total bilirubin and ammonia were measured by Van den Bergh reaction and a standard enzymatic procedure, respectively, at Oriental Kobo Life Science Laboratory.

Real-Time Reverse-Transcription PCR. Total RNA was prepared from liver tissue using RNeasy kit (QIAGEN, Tokyo, Japan). For complementary DNA synthesis, 1 μg total RNA was reverse-transcribed using the High Capacity RNA-to-DNA Master Mix (Applied Biosystems, Foster City, CA). Complementary DNA, equivalent to 40 ng RNA, was used as a template for real-time reverse-transcription PCR (RT-PCR) using an Applied Biosystems 7900HT Fast Real-Time PCR System (Applied Biosystems). The messenger RNA expressions of tumor necrosis factor alpha (TNF-α), collagen-alpha1(I), and transthyretin were measured using TaqMan Gene Expression Assays (Assay ID: Mm00443260_g1, Mm00801666_g1, and Mm00443267_m1, respectively), and were corrected with the quantified expression level of beta-actin messenger RNA measured using TaqMan Gene Expression Assays (Assay ID: Mm02619580_g1).

Statistical Analysis. Data are presented as mean ± standard deviation. Comparisons between two groups were performed by unpaired *t* test. Multiple comparisons were performed by analysis of variance followed by Scheffe *post hoc* correction. $P < 0.05$ was considered statistically significant.

Results

Hepatocyte-Specific Mcl-1 Deficiency Leads to Spontaneous Hepatocyte Apoptosis in the Adult Liver. To generate hepatocyte-specific Mcl-1–deficient mice, floxed *mcl-1* mice were crossed with heterozygous *AlbCre* mice. After *mcl-1*$^{flox/+}$ *AlbCre* mice were mated with *mcl-1*$^{flox/+}$ mice, and offspring were screened for genotyping and Mcl-1 expression. *mcl-1*$^{flox/flox}$ *AlbCre* mice were born and grew up. Their expression in the liver of Mcl-1 was greatly reduced compared with that of wild-type mice (Fig. 1A). The levels of Bcl-xL expression did not change in *mcl-1*$^{flox/flox}$ *AlbCre* liver. Bcl-xL and Mcl-1 proteins migrated as typical doublet bands of which the biochemical nature had been previously determined.[18] The trace amount of Mcl-1 expression found in the knockout liver may have been attributable to expression in nonparenchymal cells, as previously observed in hepatocyte-specific Bcl-xL–deficient mice.[13]

To investigate the significance of Mcl-1 in the liver, mice were sacrificed 6 weeks after birth and subjected to analysis of serum ALT levels and caspase-3/7 activity as well as liver histology and TUNEL staining. *mcl-1*$^{flox/flox}$ *AlbCre* mice displayed significantly higher levels of serum ALT than control mice (*AlbCre*-negative or *mcl-1*$^{+/+}$ *AlbCre* mice) (Fig. 1B). Hepatocytes with typical apoptosis morphology such as cellular shrinkage and nuclear condensation were frequently observed in the liver sections of *mcl-1*$^{flox/flox}$ *AlbCre* mice (Fig. 1C). Consistently, the number of cells with TUNEL positivity, a hallmark of apoptotic cell death, in the liver was significantly higher in *mcl-1*$^{flox/flox}$ *AlbCre* mice than in control mice (Fig. 1C). Activity of caspase-3/7, executioners of apoptosis, was significantly higher in circulation of *mcl-1*$^{flox/flox}$ *AlbCre* mice than in control mice, which might reflect activation of those proteases in the knockout liver (Fig. 1D). Bax expression was clearly increased in *mcl-1*$^{flox/flox}$ *AlbCre* mice, suggesting Bax activation being involved in the apoptosis in *mcl-1*$^{flox/flox}$ *AlbCre* mice (Fig. 1A). Furthermore, the expression of TNF-α and collagen-alpha1(I) was significantly increased in the *mcl-1*$^{flox/flox}$ *AlbCre* liver compared with the wild-type liver, as found in the Bcl-xL knockout liver (Fig. 1E). Taken together, hepatocyte-specific Mcl-1 knockout mice developed spontaneous apoptosis leading to sterile inflammation and fibrotic response in the liver, like hepatocyte-specific Bcl-xL knockout mice.[13]

Heterozygous Deletion of the mcl-1 Gene Does Not Produce Apoptosis But Increases the Susceptibility to Fas Stimulation. Although the levels of Mcl-1 expression were significantly decreased in *mcl-1*$^{flox/+}$ *AlbCre* liver (Fig. 1A, Supporting Fig. 1), *mcl-1*$^{flox/+}$ *AlbCre* mice did not have apoptosis phenotypes in the liver (Fig. 1B-D).

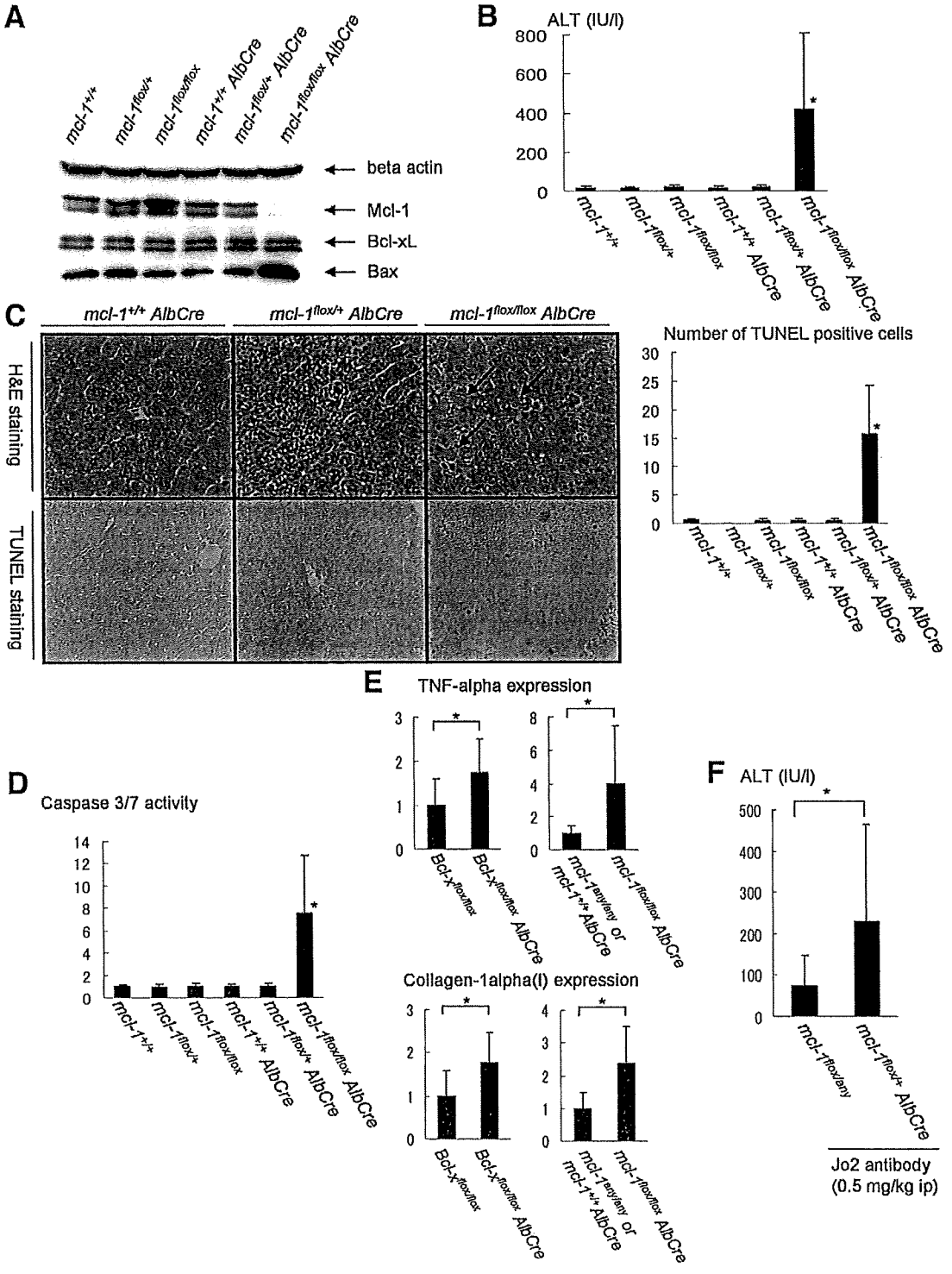

Fig. 1. Hepatocyte-specific Mcl-1 knockout mice. Offspring from mating of *mcl-1*$^{flox/+}$ *AlbCre* mice and *mcl-1*$^{flox/+}$ mice were sacrificed at the age of 6 weeks. (A) Western blot of whole liver lysate for the expression of Bcl-xL, Mcl-1, and Bax. (B) Serum ALT levels. N = 15 mice for each group. *$P < 0.05$ versus the other five groups. (C) Left panel shows hematoxylin-eosin and TUNEL staining of the liver section. Arrow indicates typical apoptotic cells. Right panel shows statistics of TUNEL-positive cells. The number of TUNEL-positive cells was determined in a defined area. N = 5 mice for each group. *$P < 0.05$ versus the other five groups. (D) Serum levels of caspase-3/7 activity. The levels were normalized to *mcl-1*$^{+/+}$ *AlbCre* (−) mice. N = 15 mice for each group. *P < 0.05 versus the other five groups. (E) Real-time RT-PCR analysis for TNF-α and collagen-1alpha(1) expression. *$P < 0.05$. N = 12 or 9. The levels were normalized to the wild-type mice. (F) Serum ALT levels of Fas-stimulated mice. The *mcl-1*$^{flox/+}$ *AlbCre* mice and *mcl-1*$^{flox/+ \text{ or } flox}$ mice were sacrificed 3 hours after intraperitoneal injection of 0.5 mg/kg Jo2 antibody. *$P < 0.05$. N = 13 or 7.

Therefore, we examined the susceptibility to Fas stimulation in these mice. We injected anti-Fas antibody into *mcl-1*$^{flox/+}$ *AlbCre* mice and *mcl-1*$^{flox/+\ or\ flox}$ mice and measured the levels of their serum ALT. *mcl-1*$^{flox/+}$ *AlbCre* mice displayed significantly higher levels of serum ALT than control mice (Fig. 1F). These findings suggest that haplo-deficiency of Mcl-1 does not produce apoptosis in a physiological setting but clearly reduces apoptosis resistance under pathological conditions.

Involvement of Bid in Apoptosis Caused by Mcl-1 Deficiency. BH3-only proteins regulate life and death balance by interacting with core Bcl-2 family members. The hepatocyte is a so-called type 2 cell, which requires Bid as a sensor for Fas-mediated apoptotic stresses.[19] In addition, it has been reported that the caspase-8/Bid pathway is involved in a variety of liver pathological conditions.[16,20] To examine the possibility of Bid being involved in hepatocyte apoptosis caused by Mcl-1 deficiency, we crossed hepatocyte-specific Mcl-1 knockout mice with Bid knockout mice. Offspring form mating of *bid*$^{+/-}$ *mcl-1*$^{flox/flox}$ *AlbCre* mice with *bid*$^{+/-}$ *mcl-1*$^{flox/flox}$ mice were sacrificed at 6 weeks after birth and subjected to analysis of apoptosis phenotypes. Mice with each genotype grew up, and, as expected, the levels of Bid and/or Mcl-1 expression in the liver were correspondingly reduced with their genotypes (Fig. 2A). The levels of serum ALT were significantly lower in *bid*$^{-/-}$ *mcl-1*$^{flox/flox}$ *AlbCre* mice than in *bid*$^{+/+}$ *mcl-1*$^{flox/flox}$ *AlbCre* mice (Fig. 2B). The results indicate that Bid was involved in hepatocyte apoptosis found in Mcl-1 knockout mice.

Combined Deficiency of Mcl-1 and Bcl-xL in Hepatocytes Causes Lethality. Phenotypes observed in hepatocyte-specific Mcl-1 knockout mice were very similar to those in hepatocyte-specific Bcl-xL knockout mice.[13] These results indicated that Bcl-xL and Mcl-1 share similar anti-apoptotic functions but do not compensate for the loss of each other. To examine whether their expression and function are completely nonredundant or just partially so, we generated hepatocyte-specific Bcl-xL/Mcl-1 double-knockout mice.

The *bcl-x*$^{flox/+}$ *mcl-1*$^{flox/+}$ *AlbCre* mice were mated with *bcl-x*$^{flox/flox}$ *mcl-1*$^{flox/flox}$ mice, and genotypes of the offspring were screened at 3 weeks after birth. *AlbCre*-negative and *bcl-x*$^{flox/+}$ *mcl-1*$^{flox/+}$ *AlbCre* mice were born and grew up, but not *bcl-x*$^{flox/flox}$ *mcl-1*$^{flox/+}$ *AlbCre*, *bcl-x*$^{flox/+}$ *mcl-1*$^{flox/flox}$ *AlbCre*, and *bcl-x*$^{flox/flox}$ *mcl-1*$^{flox/flox}$ *AlbCre* mice (Table 1). The lack of Bcl-xL and Mcl-1 caused a more severe phenotype than either knockout, suggesting that they partially compensate for the loss of each other at least from the viewpoint of maintaining normal development.

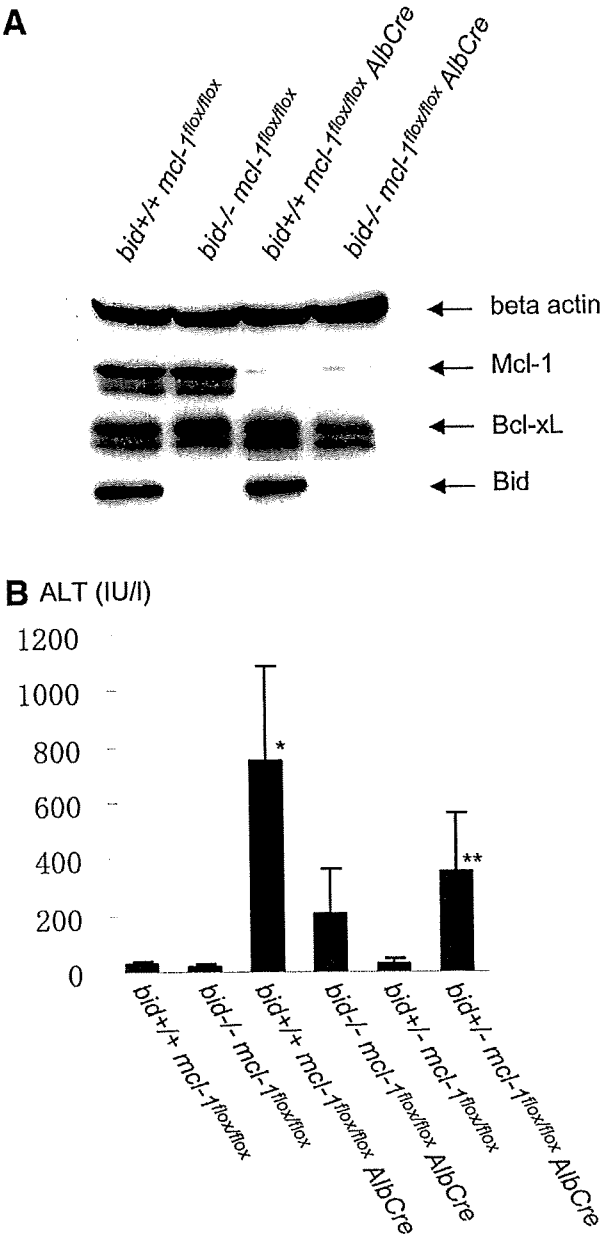

Fig. 2. Mcl-1/Bid double-knockout mice. Offspring from mating of *bid*$^{+/-}$ *mcl-1*$^{flox/flox}$ *AlbCre* mice with *bid*$^{+/-}$ *mcl-1*$^{flox/flox}$ mice were sacrificed at 6 weeks after birth. (A) Western blot of whole liver lysate for the expression of Mcl-1, Bcl-xL, and Bid. (B) Serum ALT levels. N = 12 mice for each group. *$P < 0.05$ versus the other five groups; **$P < 0.05$ versus the *AlbCre*-negative groups and the *bid*$^{+/+}$ *mcl-1*$^{flox/flox}$ *AlbCre* group.

Mice Lacking Single Alleles for Both Bcl-xL and Mcl-1 Develop Spontaneous Apoptosis in the Adult Liver Similar to Bcl-xL or Mcl-1 Knockout Mice. Offspring from mating of *bcl-x*$^{flox/+}$ *mcl-1*$^{flox/+}$ *AlbCre and bcl-x*$^{flox/flox}$ *mcl-1*$^{flox/flox}$ were sacrificed at 6 weeks after birth and subjected to analysis of Bcl-xL/Mcl-1 expression and

Table 1. Genotyping of Offspring Obtained by Crossing *bcl-x*$^{flox/+}$ *mcl-1*$^{flox/+}$ *AlbCre* Mice and *bcl-x*$^{flox/flox}$ *mcl-1*$^{flox/flox}$ Mice

AlbCre	bcl-x	mcl-1	ED18.5	3 Weeks
–	flox/+	flox/+	4	14
–	flox/flox	flox/+	6	17
–	flox/+	flox/flox	12	17
–	flox/flox	flox/flox	7	17
+	flox/+	flox/+	11	22
+	flox/flox	flox/+	8	0
+	flox/+	flox/flox	9	0
+	flox/flox	flox/flox	10	0
	Total		67	87

ED, embryonic day.

Note that each genotype is expected to account for one-eighth of the offspring from this mating.

apoptosis phenotypes. As expected, *bcl-x*$^{flox/+}$ *mcl-1*$^{flox/+}$ *AlbCre* liver expressed reduced levels of expression for both Bcl-xL and Mcl-1 (Fig. 3A). Interestingly, *bcl-x*$^{flox/+}$ *mcl-1*$^{flox/+}$ *AlbCre* mice developed spontaneous hepatocyte apoptosis as evidenced by an increase in serum ALT levels and caspase-3/7 activity (Fig. 3B,C). In agreement with this, hepatocytes with typical apoptotic morphology and positive for TUNEL staining were found scattered in the liver lobules in these mice (Fig. 3D,E). Furthermore, *bcl-x*$^{flox/+}$ *mcl-1*$^{flox/+}$ *AlbCre* mice showed higher expression of TNF-α than wild-type mice (Fig. 3F). The phenotypes were very similar to hepatocyte-specific Bcl-xL or Mcl-1knockout mice.

Hepatocyte-Specific Mcl-1/Bcl-xL-Deficient Mice Show Impaired Development of the Liver and Liver Failure During the Neonatal Period. To examine the impact of Bcl-xL/Mcl-1deficiency at an earlier time point, offspring obtained from crossing *bcl-x*$^{flox/+}$ *mcl-1*$^{flox/+}$ *AlbCre* mice and *bcl-x*$^{flox/flox}$ *mcl-1*$^{flox/flox}$ mice were analyzed on gestational day 18.5. Live-obtained embryo followed expected Mendelian frequencies (Table 1). Overall, they looked normal, and their body weight did not differ among genotypes (Fig. 4A,B). However, the livers obtained from live pups with genotype of *bcl-x*$^{flox/flox}$ *mcl-1*$^{flox/+}$ *AlbCre*, *bcl-x*$^{flox/+}$ *mcl-1*$^{flox/flox}$ *AlbCre*, or *bcl-x*$^{flox/flox}$ *mcl-1*$^{flox/flox}$ *AlbCre* were clearly smaller. The ratios of liver weight to body weight were significantly lower in those pups than in *AlbCre*-negative or *bcl-x*$^{flox/+}$ *mcl-1*$^{flox/+}$ *AlbCre* pups (Fig. 4C). The ratios of liver weight to body weight were also examined in *mcl-1*$^{flox/flox}$ with *AlbCre* or without *AlbCre* mice, and there was no significant difference between the two (6.0 ± 0.8 versus 5.5 ± 0.9, $N = 5$, $P = 0.34$), excluding the possibility that Mcl-1 knockout itself affects the liver size at this time point. Histological analysis revealed that there were a number of hepatocytes with rectangular morphology and hematopoietic cells in the developing liver of the *AlbCre*-negative pups (Fig. 4D). Whereas the number of rectangular hepatocytes in *bcl-x*$^{flox/+}$ *mcl-1*$^{flox/+}$ *AlbCre* livers was similar to that in the *AlbCre*-negative livers, it was lower in *bcl-x*$^{flox/flox}$ *mcl-1*$^{flox/+}$ *AlbCre*, *bcl-x*$^{flox/+}$ *mcl-1*$^{flox/flox}$ *AlbCre*, and *bcl-x*$^{flox/flox}$ *mcl-1*$^{flox/flox}$ *AlbCre* livers. Rectangular cells were rarely observed in *bcl-x*$^{flox/flox}$ *mcl-1*$^{flox/flox}$ *AlbCre* livers. Furthermore, the expression of albumin and transthyretin was examined in the liver as a marker for hepatocyte differentiation.[21] Consistent with histological findings, both expressions were gradually reduced from the *AlbCre*-negative livers to the *bcl-x*$^{flox/flox}$ *mcl-1*$^{flox/flox}$ *AlbCre* livers (Fig. 4E,F).

We noticed that offspring obtained from crossing *bcl-x*$^{flox/+}$ *mcl-1*$^{flox/+}$ *AlbCre* mice and *bcl-x*$^{flox/flox}$ *mcl-1*$^{flox/flox}$ mice frequently died within 1 day after birth. To examine the cause of the early neonatal death, offspring were sacrificed at 10 hours after birth. They were divided into two groups according to the data shown in Table 1: expected survivors including *AlbCre*-negative and *bcl-x*$^{flox/+}$ *mcl-1*$^{flox/+}$ *AlbCre* pups, and expected nonsurvivors including *bcl-x*$^{flox/flox}$ *mcl-1*$^{flox/+}$ *AlbCre*, *bcl-x*$^{flox/+}$ *mcl-1*$^{flox/flox}$ *AlbCre*, and *bcl-x*$^{flox/flox}$ *mcl-1*$^{flox/flox}$ *AlbCre* pups. The levels of total bilirubin and ammonia in circulation were determined and compared between the groups. Both blood bilirubin levels and ammonia levels were significantly higher in the expected nonsurvivors than in the expected survivors (Fig. 5A,B). These results suggested that *bcl-x*$^{flox/flox}$ *mcl-1*$^{flox/+}$ *AlbCre*, *bcl-x*$^{flox/+}$ *mcl-1*$^{flox/flox}$ *AlbCre*, and *bcl-x*$^{flox/flox}$ *mcl-1*$^{flox/flox}$ *AlbCre* mice died quickly after birth because of hepatic failure, in agreement with the findings of impaired liver development.

Discussion

Five members of the anti-apoptotic Bcl-2 family have been found: Bcl-2, Bcl-xL, Bcl-w, Bfl-1, and Mcl-1. Traditional knockout of Bcl-2, a prototype of this family, displays growth retardation, hair color abnormality, lymphocyte decrease, and polycystic kidney.[22,23] In agreement with the finding that Bcl-2 is not expressed in hepatocytes,[13] these mice did not show any liver phenotypes. Similarly, Bcl-w[24,25] or Bfl-1 knockout mice[26] were generated but no liver phenotypes have been reported. Traditional knockout of Bcl-xL or Mcl-1 caused more severe phenotypes. Deletion of the *bcl-x* gene resulted in embryonic lethality because of abnormal neuronal development and hematopoiesis.[27] The *mcl-1* knockout embryo fails to be implanted *in utero*.[28] Thus, study of traditional knockout mice could not reveal the significance of Bcl-xL or Mcl-1 in the liver.

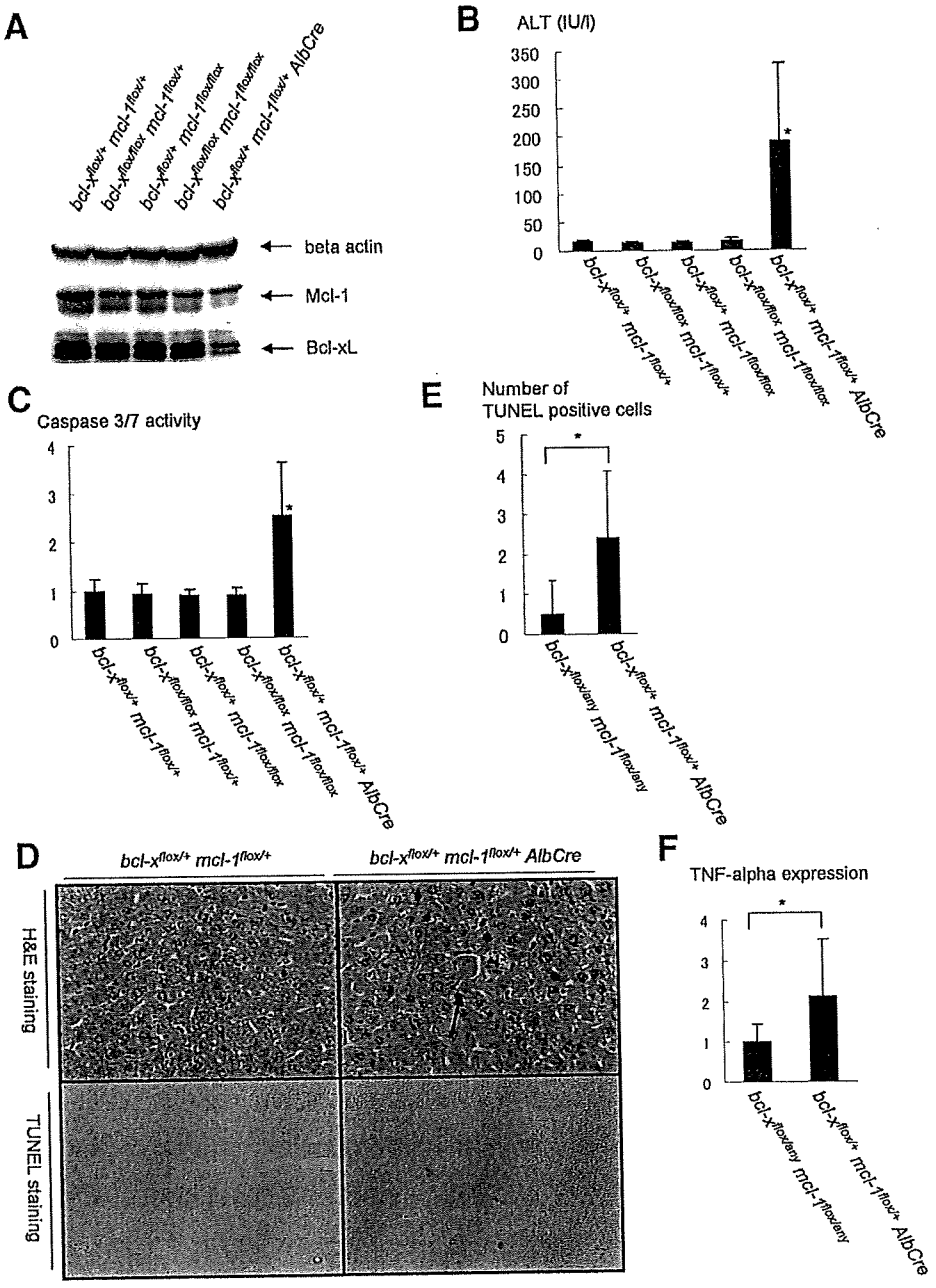

Fig. 3. Hepatocyte-specific Bcl-xL/Mcl-1-deficient mice. Offspring from mating *bcl-x*$^{flox/+}$ *mcl-1*$^{flox/+}$ *AlbCre* mice and *bcl-x*$^{flox/flox}$ *mcl-1*$^{flox/flox}$ mice were sacrificed at the age of 6 weeks. (A) Western blot of whole liver lysate for the expression of Bcl-xL and Mcl-1. (B) Serum ALT levels. N = 9 mice for each group. *$P < 0.05$ versus the other five groups. (C) Serum levels of caspase-3/7 activity. The levels were normalized to *bcl-x*$^{flox/+}$ *mcl-1*$^{flox/+}$ mice. N = 9 mice for each group. *$P < 0.05$ versus the other five groups. (D) Hematoxylin-eosin and TUNEL staining of the liver sections for *bcl-x*$^{flox/+}$ *mcl-1*$^{flox/+}$ *AlbCre* mice. Findings for *bcl-x*$^{flox/+}$ *mcl-1*$^{flox/+}$ mice are shown as a control. (E) Statistics of TUNEL-positive cells. The number of TUNEL-positive cells was determined in a defined area. N = 5 or 6. *$P < 0.05$. (F) RT-PCR analysis for TNF-α expression. The levels were normalized to the group of *bcl-x*$^{flox/+ \text{ or } flox}$ *mcl-1*$^{flox/+ \text{ or } flox}$. *$P < 0.05$. N = 9.

We previously reported that hepatocyte-specific knockout of Bcl-xL caused spontaneous apoptosis in hepatocytes after birth and established that Bcl-xL is critically important for the integrity of hepatocytes.[13] The current study demonstrated that Mcl-1 plays an anti-apoptotic role in differentiated hepatocytes similar to that of Bcl-xL. During the preparation of this manuscript, a report by Vick et al.[29] appeared on the Web, demonstrating a similar apoptosis phenotype in mice with specific knockout of the *mcl-1* gene in hepatocytes. Our findings

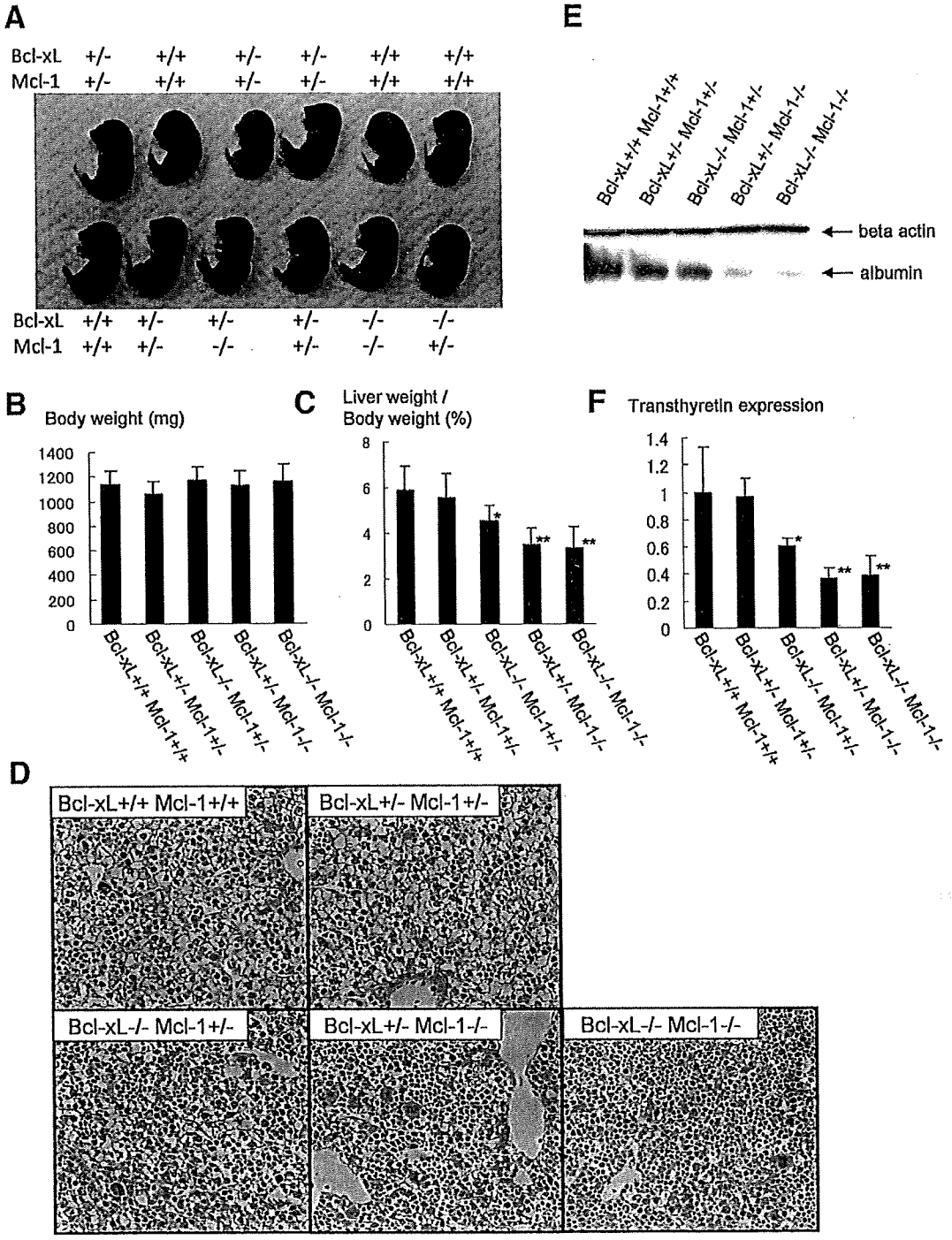

Fig. 4. Hepatocyte-specific Bcl-xL/Mcl-1-deficient embryos. Offspring from mating *bcl-x*$^{flox/+}$ *mcl-1*$^{flox/+}$ *AlbCre* mice and *bcl-x*$^{flox/flox}$ *mcl-1*$^{flox/flox}$ mice were sacrificed on day 18.5 of gestation. Mice were classified into five groups. The *bcl-x*$^{flox/+ \text{ or } flox}$ *mcl-1*$^{flox/+ \text{ or } flox}$ are indicated by Bcl-xL +/+ Mcl-1 +/+; *bcl-x*$^{flox/+}$ *mcl-1*$^{flox/+}$ *AlbCre* are indicated by Bcl-xL +/− Mcl-1 +/−; *bcl-x*$^{flox/flox}$ *mcl-1*$^{flox/+}$ *AlbCre* are indicated by Bcl-xL −/− Mcl-1 +/−; *bcl-x*$^{flox/+}$ *mcl-1*$^{flox/flox}$ *AlbCre* are indicated by Bcl-xL +/− Mcl-1 −/−; *bcl-x*$^{flox/flox}$ *mcl-1*$^{flox/flox}$ *AlbCre* are indicated by Bcl-xL −/− Mcl-1 −/ −. The numbers of embryos analyzed were 30 for Bcl-xL +/+ Mcl-1 +/+, 11 for Bcl-xL +/− Mcl-1 +/−, 8 for Bcl-xL −/− Mcl-1 +/−, 9 for Bcl-xL +/− Mcl-1 −/−, and 10 for Bcl-xL −/− Mcl-1 −/−. (A) Gross appearance of embryos. Representative photo for a litter is shown. (B) Body weight. (C) The ratios of liver weight to body weight. *$P < 0.05$ versus Bcl-xL +/+ Mcl-1 +/+; **$P < 0.05$ versus Bcl-xL +/+ Mcl-1 +/+ and Bcl-xL +/− Mcl-1 +/−. (D) Hematoxylin-eosin staining of the liver sections. (E) Western blot of whole-liver lysate for albumin expression. (F) Real-time RT-PCR analysis for transthyretin expression. The levels were normalized to the group of Bcl-xL +/+ Mcl-1 +/+. *$P < 0.05$ versus Bcl-xL +/+ Mcl-1 +/+; **$P < 0.05$ versus Bcl-xL +/+ Mcl-1 +/+ and Bcl-xL +/− Mcl-1 +/−.

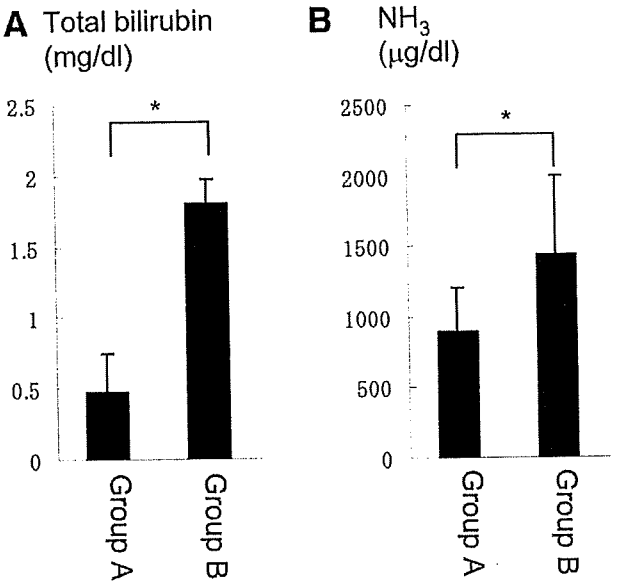

Fig. 5. Plasma biochemistry of hepatocyte-specific Bcl-xL/Mcl-1–deficient neonates 10 hours after birth. Group A (N = 13) was defined as expected survivors including *AlbCre*-negative mice and *bcl-x*$^{flox/+}$ *mcl-1*$^{flox/+}$ *AlbCre* mice. Group B (N = 6) was defined as expected nonsurvivors including *bcl-x*$^{flox/flox}$ *mcl-1*$^{flox/+}$ *AlbCre*, *bcl-x*$^{flox/+}$ *mcl-1*$^{flox/flox}$ *AlbCre*, *bcl-x*$^{flox/flox}$ *mcl-1*$^{flox/flox}$ *AlbCre*. (A) Plasma total bilirubin levels. *$P < 0.05$. (B) Plasma ammonia levels in both groups. *$P < 0.05$.

are in agreement with theirs and further provide evidence that deletion of a single allele for the *mcl-1* gene fails to produce apoptosis phenotypes under physiological conditions, as observed in knockout of the *bcl-x* gene.[13] Mcl-1 heterozygous disrupted mice did not produce apoptosis at least until 16 weeks of age (our unpublished data). It was demonstrated that hepatocyte-specific Mcl-1 knockout mice showed higher levels of liver injury than control mice on anti-Fas antibody injection.[29] However, because mice lacking both *mcl-1* alleles possess preexisting liver injury, it would be difficult to exactly compare liver injury after anti-Fas antibody injection and to conclude whether decreased Mcl-1 expression actually increases the susceptibility to Fas. In the current study, we took advantage of Mcl-1 heterozygous disrupted mice to address this point. They showed significantly higher levels of liver injury after Fas stimulation than wild-type mice, formally proving the significance of Mcl-1 expression under pathological conditions. Furthermore, our data on Mcl-1/Bid–deficient mice implies that the Bid pathway is involved in generating apoptosis found in Mcl-1 knockout mice. Because Bid mediates a variety of cellular stresses in hepatocytes upstream of Mcl-1,[30,31] it will be interesting in future study to determine what stresses generate hepatocyte apoptosis in Mcl-1 knockout mice.

Bcl-xL and Mcl-1 share similar structures and functions.[1] The observations that either deficiency similarly leads to spontaneous hepatocyte apoptosis imply that they play a non-redundant role in maintaining the integrity of hepatocytes in the adult liver. To further understand the relationship of both molecules, we generated hepatocyte-specific Bcl-xL/Mcl-1 knockout mice. Interestingly, mice lacking single alleles for both genes (*bcl-x*$^{+/-}$ *mcl-1*$^{+/-}$) induced spontaneous hepatocyte apoptosis that could not be distinguished from that found in Bcl-xL or Mcl-1 knockout mice. This indicates that, whereas knockout of a single allele of the *bcl-x* or *mcl-1* gene did not produce apoptosis, knockout of two alleles of any combination among both genes was sufficient to produce hepatocyte apoptosis. This finding suggests that both molecules are not independently but rather interdependently required for ensuring integrity of differentiated hepatocytes.

Bcl-xL/Mcl-1-deficient mice as well as mice only having a single allele of either *bcl-x* or *mcl-1* gene displayed a decreased number of hepatocytes and reduced liver size on day 18.5 of gestation and appeared to develop lethal liver failure within 1 day after birth. Because the liver contains a large number of hematopoietic cells during development (Fig. 4D), it is very difficult to determine the expression levels of Bcl-xL or Mcl-1 specifically in hepatocytes in each knockout mouse. Liver development begins on day 8.5 of gestation in the mouse when the liver primordium is delineated from the endoderm.[32] The albumin promoter, which is active in both hepatoblasts and hepatocytes, shows a 20-fold increase in transcriptional activity from day 9.5 to day 12.5 of gestation. The level of albumin then continues to increase as the liver develops simultaneously with the biliary tree and the hepatic bile duct being formed.[33] Thus, the target genes could probably be successfully deleted during embryogenesis in the *AlbCre* recombination system. The observation that Bcl-xL/Mcl-1–deficient mice developed severer phenotypes than Bcl-xL–deficient or Mcl-1–deficient mice supports the idea that Cre-mediated deletion of the target genes actually took place during embryogenesis in our model. In contrast to the knockout of two alleles, knockout of three alleles and more of the *bcl-x* and *mcl-1* genes induced lethal neonatal hepatic failure. Thus, hepatocyte integrity appeared to be strictly controlled by Bcl-xL and Mcl-1 in a gene dose–dependent manner.

Hepatocyte-specific deficiency of both Bcl-xL and Mcl-1 led to significant reduction of liver volume because of impaired hepatocyte development. However, overall, mice with these phenotypes were capable of developing normally until birth and rapidly developed liver failure and died within 1 day after birth. This finding suggests that differentiated hepatocytes are critically required for maintaining host homeostasis after birth but not during embryogenesis. The placenta

plays an important role in nutritional support and detoxification of the embryo. Our data imply that it could probably compensate for most functions of the liver cells during embryogenesis, whereas the liver would turn to the critical organ that is essential for maintaining host homeostasis after birth. Bcl-xL/Mcl-1 knockout mice provide interesting implications for the difference in the impact of differentiated hepatocytes between embryogenesis and the early neonatal period.

In conclusion, Mcl-1 and Bcl-xL are two major Bcl-2 family proteins inhibiting hepatocyte apoptosis. Together with previous work on traditional knockout mice, our data imply that other members, if any, could not compensate for their functions. Mcl-1 and Bcl-xL cooperatively maintain hepatocyte integrity during liver development and in adult liver homeostasis, and their effects are gene-dose dependent. Recent studies also have established that Mcl-1[5-7] and Bcl-xL[18,34] are frequently overexpressed and confer resistance to apoptosis in hepatocellular carcinoma. Therefore, Mcl-1 and Bcl-xL are important apoptosis antagonists in a variety of pathophysiological conditions of the liver.

Acknowledgment: We thank Dr. You-Wen He (Department of Immunology, Duke University Medical Center, Durham, NC) for providing the *mcl-1* floxed mice.

References

1. Youle RJ, Strasser A. The BCL-2 protein family: opposing activities that mediate cell death. Nat Rev Mol Cell Biol 2008;9:47-59.
2. Tsujimoto Y. Cell death regulation by the Bcl-2 protein family in the mitochondria. J Cell Physiol 2003;195:158-167.
3. Fischer U, Jänicke RU, Schulze-Osthoff K. Many cuts to ruin: a comprehensive update of caspase substrates. Cell Death Differ 2003;10:76-100.
4. Wei MC, Zong WX, Cheng EH, Lindsten T, Panoutsakopoulou V, Ross AJ, et al. Proapoptotic BAX and BAK: a requisite gateway to mitochondrial dysfunction and death. Science 2001;292:727-730.
5. Sieghart W, Losert D, Strommer S, Cejka D, Schmid K, Rasoul-Rockenschaub S, et al. Mcl-1 overexpression in hepatocellular carcinoma: a potential target for antisense therapy. J Hepatol 2006;44:151-157.
6. Fleischer B, Schulze-Bergkamen H, Schuchmann M, Weber A, Biesterfeld S, Müller M, et al. Mcl-1 is an anti-apoptotic factor for human hepatocellular carcinoma. Int J Oncol 2006;28:25-32.
7. Schulze-Bergkamen H, Fleischer B, Schuchmann M, Weber A, Weinmann A, Krammer PH, et al. Suppression of Mcl-1 via RNA interference sensitizes human hepatocellular carcinoma cells towards apoptosis induction. BMC Cancer 2006;6:232.
8. Llovet JM, Bruix J. Molecular targeted therapies in hepatocellular carcinoma. HEPATOLOGY 2008;48:1312-1327.
9. Liu L, Cao Y, Chen C, Zhang X, McNabola A, Wilkie D, et al. Sorafenib blocks the RAF/MEK/ERK pathway, inhibits tumor angiogenesis, and induces tumor cell apoptosis in hepatocellular carcinoma model PLC/PRF/5. Cancer Res 2006;66:11851-11858.
10. Casado M, Mollá B, Roy R, Fernández-Martínez A, Cucarella C, Mayoral R, et al. Protection against Fas-induced liver apoptosis in transgenic mice expressing cyclooxygenase 2 in hepatocytes. HEPATOLOGY 2007;45:631-638.
11. Schulze-Bergkamen H, Brenner D, Krueger A, Suess D, Fas SC, Frey CR, et al. Hepatocyte growth factor induces Mcl-1 in primary human hepatocytes and inhibits CD95-mediated apoptosis via Akt. HEPATOLOGY 2004;39:645-654.
12. Baskin-Bey ES, Huang W, Ishimura N, Isomoto H, Bronk SF, Braley K, et al. Constitutive androstane receptor (CAR) ligand, TCPOBOP, attenuates Fas-induced murine liver injury by altering Bcl-2 proteins. HEPATOLOGY 2006;44:252-262.
13. Takehara T, Tatsumi T, Suzuki T, Rucker EB III, Hennighausen L, Jinushi M, et al. Hepatocyte-specific disruption of Bcl-xL leads to continuous hepatocyte apoptosis and liver fibrotic responses. Gastroenterology 2004;127:1189-1197.
14. Dzhagalov I, St John A, He YW. The antiapoptotic protein Mcl-1 is essential for the survival of neutrophils but not macrophages. Blood 2007;109:1620-1626.
15. Wagner KU, Claudio E, Rucker EB 3rd, Riedlinger G, Broussard C, Schwartzberg PL, et al. Conditional deletion of the Bcl-x gene from erythroid cells results in hemolytic anemia and profound splenomegaly. Development 2000;127:4949-4958.
16. Yin XM, Wang K, Gross A, Zhao Y, Zinkel S, Klocke B, et al. Bid-deficient mice are resistant to Fas-induced hepatocellular apoptosis. Nature 1999;400:886-891.
17. Takehara T, Hayashi N, Tatsumi T, Kanto T, Mita E, Sasaki Y, et al. Interleukin 1β protects mice from Fas-mediated hepatocyte apoptosis and death. Gastroenterology 1999;117:661-668.
18. Takehara T, Takahashi H. Suppression of Bcl-xL deamidation in human hepatocellular carcinomas. Cancer Res 2003;63:3054-3057.
19. Scaffidi C, Fulda S, Srinivasan A, Friesen C, Li F, Tomaselli KJ, et al. Two CD95 (APO-1/Fas) signaling pathways. EMBO J 1998;17:1675-1687.
20. Faubion WA, Guicciardi ME, Miyoshi H, Bronk SF, Roberts PJ, Svingen PA, et al. Toxic bile salts induce rodent hepatocyte apoptosis via direct activation of Fas. J Clin Invest 1999;103:137-145.
21. Tosh D, Shen CN, Slack JM. Differentiated properties of hepatocytes induced from pancreatic cells. HEPATOLOGY 2002;36:534-543.
22. Veis DJ, Sorenson CM, Shutter JR, Korsmeyer SJ. Bcl-2-deficient mice demonstrate fulminant lymphoid apoptosis, polycystic kidneys, and hypopigmented hair. Cell 1993;75:229-240.
23. Nakayama K, Nakayama K, Negishi I, Kuida K, Sawa H, Loh DY. Targeted disruption of Bcl-2 alpha beta in mice: occurrence of gray hair, polycystic kidney disease, and lymphocytopenia. Proc Natl Acad Sci U S A 1994;91:3700-3704.
24. Print CG, Loveland KL, Gibson L, Meehan T, Stylianou A, Wreford N, et al. Apoptosis regulator bcl-w is essential for spermatogenesis but appears otherwise redundant. Proc Natl Acad Sci U S A 1998;95:12424-12431.
25. Ross AJ, Waymire KG, Moss JE, Parlow AF, Skinner MK, Russell LD, et al. Testicular degeneration in Bclw-deficient mice. Nat Genet 1998;18:251-256.
26. Hamasaki A, Sendo F, Nakayama K, Ishida N, Negishi I, Nakayama K, et al. Accelerated neutrophil apoptosis in mice lacking A1-a, a subtype of the bcl-2-related A1 gene. J Exp Med 1998;188:1985-1992.
27. Motoyama N, Wang F, Roth KA, Sawa H, Nakayama K, Nakayama K, et al. Massive cell death of immature hematopoietic cells and neurons in Bcl-x-deficient mice. Science 1995;267:1506-1510.
28. Rinkenberger JL, Horning S, Klocke B, Roth K, Korsmeyer SJ. Mcl-1 deficiency results in peri-implantation embryonic lethality. Genes Dev 2000;14:23-27.
29. Vick B, Weber A, Urbanik T, Maass T, Teufel A, Krammer PH, et al. Knockout of myeloid cell leukemia-1 induces liver damage and increases apoptosis susceptibility of murine hepatocytes. HEPATOLOGY 2009;49:627-636.
30. Yin XM. Bid, a BH3-only multi-functional molecule, is at the cross road of life and death. Gene 2006;369:7-19.
31. Malhi H, Gores GJ. Cellular and molecular mechanisms of liver injury. Gastroenterology 2008;134:1641-1654.
32. Kaestner KH. The making of the liver: developmental competence in foregut endoderm and induction of the hepatogenic program. Cell Cycle 2005;4:146-1148.
33. Cascio S, Zaret KS. Hepatocyte differentiation initiates during endodermal-mesenchymal interactions prior to liver formation. Development 1991;113:217-225.
34. Takehara T, Liu X, Fujimoto J, Friedman SL, Takahashi H. Expression and role of Bcl-xL in human hepatocellular carcinomas. HEPATOLOGY 2001;34:55-61.

Case report

Two types of drug-resistant hepatitis B viral strains emerging alternately and their susceptibility to combination therapy with entecavir and adefovir

*Nao Kurashige[1], Kazuyoshi Ohkawa[1], Naoki Hiramatsu[1], Tsugiko Oze[1], Takayuki Yakushijin[1], Kiyoshi Mochizuki[1], Atsushi Hosui[1], Takuya Miyagi[1], Hisashi Ishida[1], Tomohide Tatsumi[1], Tatsuya Kanto[1], Tetsuo Takehara[1] and Norio Hayashi[1]**

[1]Department of Gastroenterology and Hepatology, Osaka University Graduate School of Medicine, Suita, Osaka, Japan

*Corresponding author: e-mail: hayashin@gh.med.osaka-u.ac.jp

The most serious problem of nucleoside/nucleotide analogue therapy for hepatitis B virus (HBV) infection is the emergence of drug-resistant mutant virus. Here, we describe a patient with chronic hepatitis B infection with a complex drug-resistant mutant virus during sequential therapy with lamivudine (3TC), entecavir (ETV) and adefovir dipivoxil (ADV). The patient was a 52-year-old male with positive hepatitis B e antigen and high HBV DNA (>7.6 $\log_{10}$ copies/ml). Initial 3TC monotherapy offered little benefit and 3TC resistance was established by the virus with rtA181T and not rtM204V/I. HBV DNA was reduced slightly by replacement with ETV monotherapy and was followed by virological breakthrough. At that time, rtA181T was undetectable and the virus with rtM204V and rtL180M became predominant. ETV resistance was established by an additional rtS202G mutation. Efficacy of subsequent combination therapy with ADV and 3TC was limited because of reappearance of the virus with rtA181T, which might confer cross-resistance to 3TC and ADV. Final combination therapy with ETV and ADV reduced HBV DNA to 3.7 $\log_{10}$ copies/ml for 5 months, which was the most effective therapy for this patient. Thus, two kinds of mutant viruses (rtM204V-related and rtA181T-related) appeared alternately in this patient. Combination therapy with ETV and ADV might have been effective because these drugs share therapeutic roles, that is, ETV affects the rtA181T-related virus and ADV affects the rtM204V-related virus. This is the first report suggesting clinical significance of combination therapy with ETV and ADV for controlling replication of the complex drug-resistant mutant HBV.

Introduction

Nucleoside/nucleotide analogues have a better therapeutic effect on chronic hepatitis B virus (HBV) infection than previously used drugs. They strongly suppress HBV replication and retard disease progression [1,2]; however, the most serious problem associated with nucleoside/nucleotide analogues is the emergence of drug-resistant viruses through long-term administration. Drug-resistant viruses for nucleoside/nucleotide analogues occur as a result of amino acid substitutions within the reverse transcriptase (RT) domain of the HBV polymerase gene. Lamivudine (3TC) resistance is primarily caused by mutations rtM204V/I and rtL180M, the latter of which is a compensatory substitution [3,4]. Adefovir dipivoxil (ADV) resistance is associated with the mutations rtA181V/T and/or rtN236T [5]. Entecavir (ETV) resistance is established by substitution(s) at rt184, rt202 and/or rt250 in addition to 3TC-resistant substitutions, rtM204V and rtL180M [6].

Recently, the substitution at rt181 has been reported to confer cross-resistance not only to ADV, but also to other nucleoside/nucleotide analogues [7,8]. Some investigators have suggested that 3TC resistance can occur not only with rtM204V/I, but also with rtA181T [9,10]. A more recent report has shown that rtA181V/T is involved in resistance to multiple drugs, including 3TC, ADV and tenofovir disoproxil fumarate, although the degree of drug resistance varies considerably among HBV strains *in vitro* [8].

In this report, we describe a chronic HBV patient who has a complex drug-resistant mutant virus that was identified during sequential therapy with three nucleoside/nucleotide analogues. In this patient, two kinds of mutant viral strains based on the rtM204V and

rtA181T substitutions appeared alternately. We also refer to the clinical usefulness of combination therapy with ETV and ADV for the mutant HBV strain.

Patient clinical course

The patient was a 52-year-old male who first visited Osaka University Hospital (Osaka, Japan) in September 2004. He had been diagnosed as a chronic HBV carrier 5 years earlier. He was a chronic drinker, with alcohol consumption of approximately 65 g/day. He had also suffered from type-2 diabetes mellitus for >10 years and had undergone insulin therapy for 10 months. The laboratory data at his first visit were alanine aminotransferase (ALT) 68 IU/l (normal level ≤40 IU/l), aspartate aminotransferase (AST) 75 IU/l (normal level ≤40 IU/l), γ-glutamyl transpeptidase (GGT) 189 IU/l (normal level <50 IU/l), fasting plasma glucose (FPG) 239 mg/dl (normal level ≤110 mg/dl), glycated haemoglobin (HbA1c), 10.3% (normal range 4.3–5.8%) and HBV DNA>7.6 $\log_{10}$ copies/ml. Hepatitis B surface antigen (HBsAg) and hepatitis B e antigen (HBeAg) were positive, whereas antibodies against HBsAg (anti-HBs), HBeAg (anti-HBe), hepatitis C virus and HIV were negative. Liver histology showed mild piecemeal necrosis, mild lobular inflammation and mild portal fibrosis; however, steatosis was found in only <5% of the hepatocytes. 3TC (100 mg/day) therapy was commenced in October 2004. Sequencing analysis before therapy revealed no drug-resistance-associated mutations. After starting 3TC therapy, HBV DNA decreased to 6.5 $\log_{10}$ copies/ml in February 2006 and increased again to >7.6 $\log_{10}$ copies/ml in April 2006. ALT levels were almost abnormal and on one occasion flared up to 472 IU/l in December 2005 despite cessation of drinking. rtM204V/I was not detected by repeated PCR-enzyme-linked minisequence assay [11], but rtA181T was found by sequencing analysis in October 2006. At this point, 3TC was switched to ETV monotherapy (0.5 mg/day). The laboratory data at the beginning of ETV administration were ALT 64 IU/l, AST 78 IU/l, GGT 268 IU/l and HBV DNA>7.6 $\log_{10}$ copies/ml. Diabetes mellitus was improved (FPG 123 mg/dl and HbA1c 6.9%) because of a strict diet. During ETV therapy, HBV DNA decreased to 5.6 $\log_{10}$ copies/ml in February 2007, but virological breakthrough was observed in August 2007 (HBV DNA 6.7 $\log_{10}$ copies/ml). As for drug-resistance-associated mutations, rtM204V and rtL180M were detected in September 2007, and rtS202G was detected in January 2008 despite an increasing dose of ETV (1 mg/day). ETV administration was stopped in March 2008 and replaced by combination therapy of 3TC (100 mg/day) with ADV (10 mg/day). The laboratory data at that time were ALT 29 IU/l, AST 49 IU/l, GGT 161 IU/l and HBV DNA 7.0 $\log_{10}$ copies/ml. The combination therapy led to a slight decrease in HBV DNA to 5.6 $\log_{10}$ copies/ml in June 2008. In September 2008, rtA181T was detected again, whereas rtL180M, rtS202G and rtM204V were not detected. From October 2008, a combination therapy with ADV (10 mg/day) and ETV (0.5 mg/day) was carried out. HBV DNA decreased from 5.8 to 3.7 $\log_{10}$ copies/ml for 5 months.

In this patient, ALT fluctuated within the normal to slightly abnormal range (≤60 IU/l) during ETV monotherapy and subsequent combination therapy. Improvement of liver function was observed despite poor control of HBV replication and appeared to be greatly attributed to recovery from alcoholic and diabetes mellitus-related liver diseases. Throughout the follow-up period, no side effects from the nucleoside/nucleotide analogues were observed. The clinical course of the patient is summarized in Figure 1.

Serological and virological assays for HBV

HBsAg, anti-HBs, HBeAg and anti-HBe were determined by chemiluminescent immunoassays. HBV DNA was quantified by a PCR-based method (Amplicor HBV monitor; Roche Diagnostics, Basel, Switzerland). The 3TC-resistant rtM204V/I substitution was examined by PCR-enzyme-linked minisequence assay [11]. Nucleotide sequences of the entire RT region were determined by PCR direct sequencing. The primers BF5 (5′-AAGAGACAGTC ATCCTCAGG-3′, nucleotides 3183–3202) and BR8 (5′-TTGCGTCAGCAAACACTTGG-3′, nucleotides 1195–1176) were used for the amplification. The sequencing analyses were done using sera collected in October 2004, October 2006, September 2007, January 2008 and September 2008 (designated as P1 to P5, respectively; Figure 1).

Results of sequencing analyses

Sequencing data showed that the patient was infected with HBV genotype C according to phylogenetic tree analysis (data not shown). The results of serial sequencing analyses from P1 to P5 are shown in Figure 2. The virus with rtA181T and rtF221Y was detected at P2. By contrast, the virus with rtL180M, rtM204V, rtL229V and rtL269I became predominant at P3. At P4, rtS202G was added, although it occurred incompletely; however, the dominant virus at P5 possessed rtA181T and rtF221Y and was identical to that at P2.

We also compared HBV DNA sequences around rt180 and rt181 obtained at P1–P5 (Figure 3). At P2 and P5, two types of mutations were identified: one was an A670 mutation causing rtA181T and an in-frame stop codon formation at codon 172 of the *S* gene, and

the other was a C669/A670 double mutation, which resulted in rtA181 but avoided the stop codon formation in the *S* gene. At P3 and P4, the A667 mutation, which led to rtL180M, was detected.

Discussion

In this paper, we have described a chronic hepatitis B patient with a complex drug-resistant mutant virus. In this patient, initial 3TC monotherapy offered little benefit and virological breakthrough was observed after administration. 3TC resistance was not caused by rtM204V/I but by rtA181T. After 3TC was replaced by ETV, HBV DNA decreased to 5.6 $\log_{10}$ copies/ml, followed by virological breakthrough for a short period of time. At that time, rtA181T was not detected, and the virus with rtM204V and rtL180M was predominant. This indicates that the virus with rtM204V and rtL180M might have already coexisted as a minor population before ETV therapy, and that the virus with rtA181T might have been reduced because of its susceptibility to ETV. Indeed, the virus with rtA181V/T has been reported to be sensitive to ETV *in vitro* [8]. The ETV resistance-specific rtS202G was not yet seen at the time of virological breakthrough. It was observed a short time later, resulting in the establishment of ETV resistance, although the reasons for virological breakthrough prior to the detection of the ETV-resistant HBV strain remains to be understood.

Subsequently, combination therapy with ADV and 3TC was done because ADV has been reported to have an effect on ETV resistance [12,13]; however, its efficacy was limited and the virus with rtA181T reappeared. The virus with rtM204V, rtL180M and rtS202G became undetectable. This might be because the virus with rtM204V, rtL180M and rtS202G was susceptible

Figure 1. Clinical course of a patient with a complex drug-resistant mutant HBV during sequential therapy with 3TC, ETV and ADV

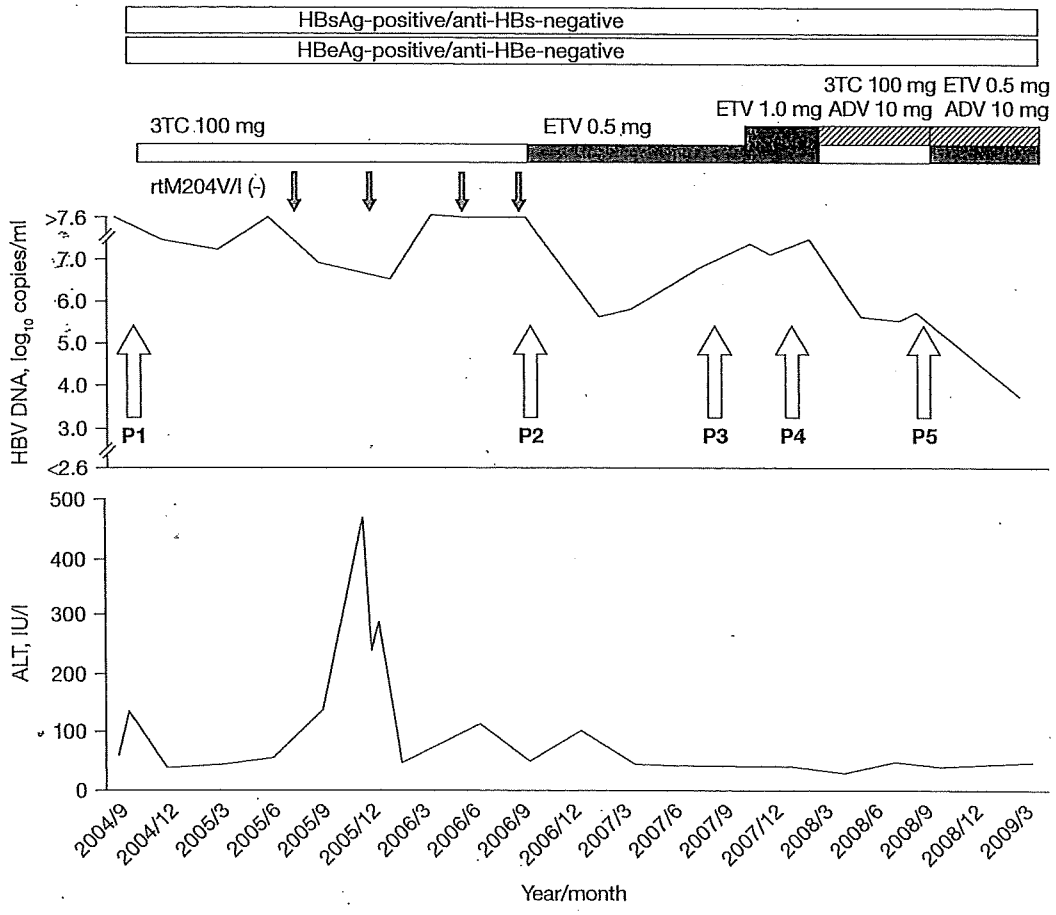

Black arrows represent the absence of the rtM204V/I substitution as detected by PCR-enzyme-linked minisequence assay. White arrows represent the serum sampling points (October 2004, October 2006, September 2007, January 2008 and September 2008 designated as P1 to P5, respectively) for sequencing analysis of the hepatitis B virus (HBV) reverse transcriptase region. ADV, adefovir dipivoxil; ALT, alanine aminotransferase; anti-HBe, antibodies against hepatitis B e antigen; anti-HBs, antibodies against hepatitis B surface antigen; ETV, entecavir; HBeAg, hepatitis B e antigen; HBsAg, hepatitis B surface antigen; 3TC, lamivudine.

Figure 2. Amino acid sequences of the RT region of the HBV polymerase gene at serum sampling points P1–P5

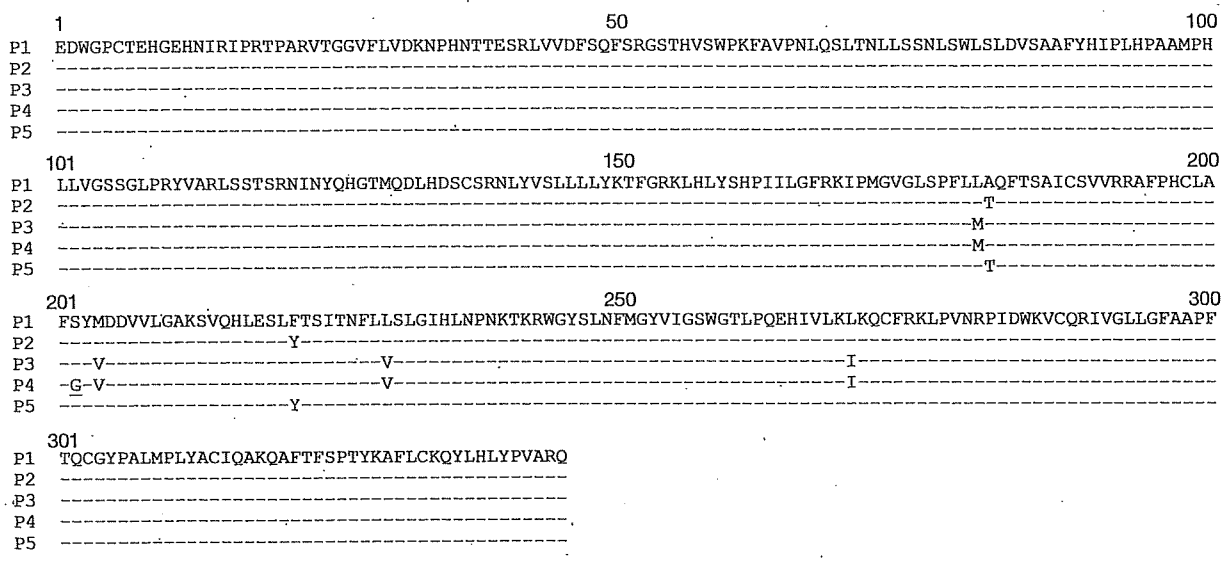

An amino acid residue identical to that of the top sequence is shown by dashes. The underlined residue indicates the coexistence with the identical residue to the top sequence. Sampling points were at October 2004, October 2006, September 2007, January 2008 and September 2008 (designated as P1 to P5, respectively). HBV, hepatitis B virus; RT, reverse transcriptase.

Figure 3. DNA and amino acid sequences around the positions rt180 and rt181 at serum sampling points P1–P5

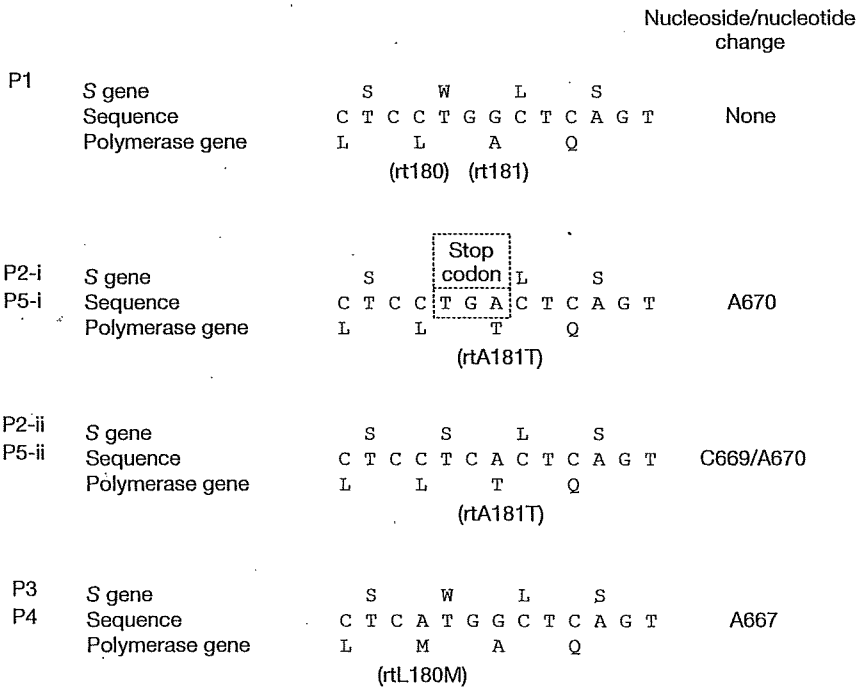

Mutated nucleosides/nucleotides and substituted amino acid residues are underlined. As for nucleoside/nucleotide changes, the nucleoside/nucleotide numbering is according to the representative hepatitis B virus (HBV) genotype C strain (GenBank accession number AB033550) [15], where position 1 is an *EcoR*I recognition site. Sampling points were at October 2004, October 2006, September 2007, January 2008 and September 2008 (designated as P1 to P5, respectively).

to ADV, whereas the virus with rtA181T revealed resistance to 3TC and possibly ADV. Final combination therapy with ETV and ADV resulted in a decrease in HBV DNA to 3.7 $\log_{10}$ copies/ml for 5 months, which was the most effective therapeutic regimen for this patient. Thus, two kinds of drug-resistant viral strains, the rtA181T-related strain and the rtM204V-related strain, appeared alternately in this patient. It is noteworthy that combination therapy with ETV and ADV was effective against such a complex mutant HBV. This might be because of the sharing of therapeutic roles of these drugs: ETV for the rtA181T-related strain and ADV for the rtM204V-related strain.

rtA181T, which is generally caused by the A670 mutation, results in the in-frame stop codon formation at codon 172 of the *S* gene. In this patient, the virus with the C669/A670 double mutation, which could produce the surface protein, coexisted with the virus with the A670 mutation alone. A similar virus with the T669/A670 double mutation, which compensates for the defect of surface protein production, has also been reported [7,14].

In summary, we have reported on a complex drug-resistant mutant HBV related to both rtA181T and rtM204V substitutions in a patient with chronic HBV, who received sequential therapy of nucleoside/nucleotide analogues. We also showed for the first time that combination therapy with ETV and ADV might be of clinical significance for controlling replication of complex mutant HBV.

Disclosure statement

The authors declare no competing interests.

References

1. Lavanchy D. Hepatitis B virus epidemiology, disease burden, treatment, and current and emerging prevention and control measures. *J Viral Hepat* 2004; 11:97–107.
2. Keeffe EB, Dieterich DT, Han SHB, *et al.* A treatment algorithm for the management of chronic hepatitis B virus infection in the United States: 2008 update. *Clin Gastroenterol Hepatol* 2008; 6:1315–1341.
3. Allen MI, Deslauriers M, Andrews CW, *et al.* Identification and characterization of mutations in hepatitis B virus resistant to lamivudine. *Hepatology* 1998; 27:1670–1677.
4. Liaw YF, Chien RN, Yeh CT, Tsai SL, Chu CM. Acute exacerbation and hepatitis B virus clearance after emergence of YMDD motif mutation during lamivudine therapy. *Hepatology* 1999; 30:567–572.
5. Hadziyannis SJ, Tassopoulos NC, Heathcote EJ, *et al.* Long-term therapy with adefovir dipivoxil for HBeAg-negative chronic hepatitis B for up to 5 years. *Gastroenterology* 2006; 131:1743–1751.
6. Tenney DJ, Rose RE, Baldick CJ, *et al.* Two-year assessment of entecavir resistance in lamivudine-refractory hepatitis B virus patients reveals different clinical outcomes depending on the resistance substitutions present. *Antimicrob Agents Chemother* 2007; 51:902–911.
7. Yatsuji H, Noguchi C, Hiraga N, *et al.* Emergence of a novel lamivudine-resistant hepatitis B virus variant with a substitution outside the YMDD motif. *Antimicrob Agents Chemother* 2006; 50:3867–3874.
8. Villet S, Pichoud C, Billioud G, *et al.* Impact of hepatitis B virus rtA181V/T mutants on hepatitis B treatment failure. *J Hepatol* 2008; 48:747–755.
9. Yeh CT, Chien RN, Chu CM, *et al.* Clearance of the original hepatitis B virus YMDD-motif mutants with emergence of distinct lamivudine-resistant mutants during prolonged lamivudine therapy. *Hepatology* 2000; 31:1318–1326.
10. Pai SB, Bozdayi AM, Pai RB, *et al.* Emergence of a novel mutation in the FLLA region of hepatitis B virus during lamivudine therapy. *Antimicrob Agents Chemother* 2005; 49:2618–2624.
11. Kobayashi S, Ide T, Sata M. Detection of YMDD motif mutations in some lamivudine-untreated asymptomatic hepatitis B virus carriers. *J Hepatol* 2001; 34:584–586.
12. Villet S, Ollivet A, Pichoud C, *et al.* Stepwise process for the development of entecavir resistance in a chronic hepatitis B virus infected patient. *J Hepatol* 2007; 46:531–538.
13. Yatsuji H, Hiraga N, Mori N, *et al.* Successful treatment of an entecavir-resistant hepatitis B virus variant. *J Med Virol* 2007; 79:1811–1817.
14. Yatsuji H, Suzuki F, Sezaki H, *et al.* Low risk of adefovir resistance in lamivudine-resistant chronic hepatitis B patients treated with adefovir plus lamivudine combination therapy: two-year follow-up. *J Hepatol* 2008; 48:923–931.
15. Okamoto H, Tsuda F, Sakugawa H, *et al.* Typing hepatitis B virus by homology in nucleotide sequence: comparison of surface antigen subtypes. *J Gen Virol* 1988; 69:2575–2583.

Accepted for publication 24 May 2009